NeuroImage 134 (2016) 630–644

Contents lists available at ScienceDirect

NeuroImage

journal homepage: www.elsevier.com/locate/ynimg

Auditory motion in the sighted and blind: Early visual deprivation triggers a large-scale imbalance between auditory and "visual" brain regions

Giulia Dormal [a,b,c,*,1], Mohamed Rezk [d,1], Esther Yakobov [e], Franco Lepore [a], Olivier Collignon [d,**]

[a] Centre de recherche en Neuropsychologie et Cognition (CERNEC), University of Montreal, Canada
[b] Institut de Psychologie et Institut de Neurosciences, University of Louvain, Belgium
[c] Biological Psychology and Neuropsychology, Institute for Psychology, University of Hamburg, Germany
[d] Centre for Mind/Brain Science (CIMeC), University of Trento, Italy
[e] Department of Psychology, McGill University, Canada

ARTICLE INFO

Article history:
Received 7 September 2015
Revised 31 March 2016
Accepted 13 April 2016
Available online 20 April 2016

Keywords:
Blindness
Crossmodal plasticity
Motion processing
In-depth motion
Lateral motion
hMT+/V5

ABSTRACT

How early blindness reorganizes the brain circuitry that supports auditory motion processing remains controversial. We used fMRI to characterize brain responses to in-depth, laterally moving, and static sounds in early blind and sighted individuals. Whole-brain univariate analyses revealed that the right posterior middle temporal gyrus and superior occipital gyrus selectively responded to both in-depth and laterally moving sounds only in the blind. These regions overlapped with regions selective for visual motion (hMT+/V5 and V3A) that were independently localized in the sighted. In the early blind, the right planum temporale showed enhanced functional connectivity with right occipito-temporal regions during auditory motion processing and a concomitant reduced functional connectivity with parietal and frontal regions. Whole-brain searchlight multivariate analyses demonstrated higher auditory motion decoding in the right posterior middle temporal gyrus in the blind compared to the sighted, while decoding accuracy was enhanced in the auditory cortex bilaterally in the sighted compared to the blind. Analyses targeting individually defined visual area hMT+/V5 however indicated that auditory motion information could be reliably decoded within this area even in the sighted group. Taken together, the present findings demonstrate that early visual deprivation triggers a large-scale imbalance between auditory and "visual" brain regions that typically support the processing of motion information.

1. Introduction

Area hMT+/V5 is classically considered to support motion processing based on visual inputs only (Watson et al., 1993; Tootell et al., 1995). However, previous studies have shown that this region selectively responds to auditory (Poirier et al., 2006; Bedny et al., 2010; Wolbers et al., 2011; Strnad et al., 2013; Jiang et al., 2014) and tactile motion (Ricciardi et al., 2007) in individuals with early-onset blindness. Whether this non-visual recruitment of hMT+/V5 is specific to the blind due to crossmodal plasticity or could also be observed in sighted individuals remains currently debated. The answer to this question is crucial to unravel the role of developmental vision in shaping the modality tuning of area hMT+/V5 for motion processing. Some studies have shown that auditory (Warren et al., 2002; Poirier et al., 2005; Alink et al., 2008; Strnad et al., 2013) and tactile (Hagen et al., 2002; Blake et al., 2004; Beauchamp et al., 2007; Ricciardi et al., 2007; Summers et al., 2009; van Kemenade et al., 2014) motion also involves part of hMT+/V5 in sighted individuals. Based on these findings, it was suggested that part of hMT+/V5 may act as a supramodal region for motion computation and develop independently of visual experience (Pascual-Leone and Hamilton, 2001; Ricciardi et al., 2007; Ricciardi and Pietrini, 2011). Other studies however failed to identify a crossmodal involvement of area hMT+/V5 in non-visual motion processing in the sighted (Lewis et al., 2000; Bremmer et al., 2001; Saenz et al., 2008; Bedny et al., 2010; Alink et al., 2011; Jiang et al., 2014, 2015).

Inconsistencies across studies may stem from a variety of parameters such as the sensory modality investigated (audition vs. touch), the specific features of the stimuli, and the experimental paradigm itself (e.g. block vs. event-related design). The choice of analytical steps, such as the use of univariate vs. multivariate analyses and the investigation of whole-brain vs. region-of-interest (ROI) analytic space, may also lead to different conclusions. For example, Bedny et al. (2010) found auditory motion responses in hMT+/V5 in congenitally blind but not in sighted

* Correspondence to: G. Dormal, Biological Psychology and Neuropsychology, Institute for Psychology, University of Hamburg, Von-Melle-Park 11, 20146 Hamburg, Germany.
** Correspondence to: O. Collignon, Center for Mind/BrainSciences (CIMeC), Via delle Regole 101, 38060 Mattarello, Italy.
E-mail addresses: giulia.dormal@uni-hamburg.de (G. Dormal), olivier.collignon@unitn.it (O. Collignon).
[1] These authors contributed equally.

http://dx.doi.org/10.1016/j.neuroimage.2016.04.027
1053-8119/

subjects when using a univariate approach. However, multivariate pattern analyses conducted on the same dataset revealed that auditory motion could be decoded significantly above chance level in this area in both groups (Strnad et al., 2013).

While the latter study and previous work (e.g. Blake et al., 2004; Wolbers et al., 2011; Jiang et al., 2014) focused on area hMT+/V5 as a region of interest, a whole-brain analytic approach is necessary to ascertain that auditory motion processing specifically maps in this area. The presence of auditory motion information in occipito-temporal regions outside of the typical visual-motion network would challenge the idea of a topological selectivity for auditory motion processing in the occipito-temporal cortex. Indeed, some studies suggested that response preference to auditory motion is widespread across the occipital cortex of blind individuals rather than localized in specific regions (Poirier et al., 2006; Lewald and Getzmann, 2013). Importantly, whole-brain imaging also allows investigating how the crossmodal recruitment of the occipital cortex during auditory motion processing in the early blind affects brain circuits typically dedicated to this input and function *outside* of the occipital cortex. Some evidence points to the presence of plastic changes within the cortices subtending the preserved non-visual modalities in early blind subjects. For instance, blind show enlarged tonotopic maps (Sterr et al., 1998a,b; Elbert et al., 2002) and enhanced voice selective activity (Gougoux et al., 2009) in temporal regions. In contrast, occipital crossmodal recruitment in the blind during auditory, haptic and even language processing can be associated with a *reduced* responsiveness of non-visual areas that typically support these inputs/functions (Cohen et al., 1997; Amedi et al., 2004; Collignon et al., 2009a; Stevens and Weaver, 2009; Jiang et al., 2014; Hölig et al., 2014; Bedny et al., 2015). Hence, whether intramodal plasticity in the cortices that support the preserved non-visual modalities in the early blind emerges as increases or decreases in responsiveness remains debated.

The main goals of the present study were twofold. First, we aimed at clarifying whether crossmodal responses to non-visual motion are specific to the early blind and whether these responses are confined to brain regions that typically support visual motion processing in sighted individuals. Second, we aimed at characterizing how early blindness affects the responsiveness and the connectivity of brain regions outside of the deprived "visual" cortex during auditory motion processing.

For this purpose, we investigated auditory motion selectivity in early blind and sighted subjects using both univariate and multivariate whole-brain analyses. Analyses within individually-defined regions of interest were additionally carried out in the sighted in order to further test the presence of auditory motion information in visual area hMT+/V5. We used 2 types of auditory motion trajectories, in-depth and lateral motion, since there is evidence that distinct neural populations respond to these motion trajectories both in audition (Stumpf et al., 1992; Toronchuk et al., 1992) and vision (radial and translational motion) (Saito et al., 1986; Tanaka and Saito, 1989; Morrone et al., 2000).

2. Materials and methods

2.1. Participants

Sixteen early blind and 15 sighted subjects (matched to the blind group for age, gender, handedness, educational level and musical experience) participated in this study. Blind participants were either totally blind or had only rudimentary sensitivity for brightness differences and no pattern vision. In all cases, blindness was attributed to peripheral deficits with no neurological impairment (Supplementary Table 1). All the procedures were approved by the research ethic and scientific boards of the "Centre for Interdisciplinary Research in Rehabilitation of Greater Montreal (CRIR)" and the "Quebec Bio-Imaging Network (QBIN)". Experiments were undertaken with the consent of each participant.

Of the 31 participants recruited for the study, 4 participants in total were judged as outliers based on their target detection performance (hits − false alarms) as it was lower than the average of the subjects in the same group by more than 2 standard deviations. We decided to exclude these participants from the analyses since we could not guarantee that they understood the task and paid sufficient attention to the stimuli. Three participants (1 blind, 2 sighted) were excluded from the analyses in the auditory experiment, and two participants were excluded from the analyses in the visual experiment. A total of 28 participants were therefore included in the analyses in the auditory experiment: 15 early blind participants (5 females, range = 23 to 62 years, mean ± SD = 44.8 ± 12.6 years) and 13 sighted participants (4 females, range = 22 to 56 years, mean ± SD = 41.6 ± 10.7 years). A total of 13 sighted participants were included in the analyses in the visual experiment (4 females, range 22 to 56 years, mean ± SD = 40.6 ± 11 years).

2.2. Task and general experimental design

Participants in both groups were scanned in one auditory run of 390 brain volumes (TR = 2200 ms) and were blindfolded throughout the fMRI acquisition. Sighted participants were additionally scanned in one visual run of 410 brain volumes (TR = 2200 ms) on a separate day. In order to familiarize the participants to the fMRI environment before the fMRI acquisition, participants underwent a training session in a mock scanner. During that session participants practiced the tasks in the bore of the simulator while listening to recorded scanner sounds. In the scanner, auditory stimuli were delivered by means of circumaural, fMRI-compatible headphones (Mr Confon, Magdeburg, Germany). Visual stimuli were projected on a screen at the back of the scanner and visualized through a mirror (127 mm × 102 mm) that was mounted at a distance of approximately 12 cm from the eyes of the participants.

2.2.1. Auditory experiment

Auditory stimuli consisted of pink noise sounds from 3 different categories: (1) in-depth motion, (2) lateral motion, and (3) stationary sounds (no motion) (Fig. 1A). In line with other neuroimaging studies of auditory motion processing (Griffiths and Green, 1999; Warren et al., 2002; Saenz et al., 2008; Alink et al., 2011; Saldern and Noppeney, 2013), we used the broadband pink noise sounds (44.1 Hz sampling rate) as they match the spectrum of frequencies most commonly heard in the everyday world without referring to a specific object. Additionally, pink noise minimizes the possibility that a putative occipital response in sighted subjects is a consequence of visual imagery. Moreover, pilot experiments in the scanner revealed that pink noises provided a more vivid sensation of motion relative to pure tones. Sounds lasted either 1 s (standard) or 1.8 s (target) in duration. In the in-depth motion condition, sounds (mono) either rose or decreased exponentially in intensity (from 10% to maximal intensity and from maximal intensity to 10% intensity) creating the vivid perception of a sound moving toward or away from the listener. In the lateral motion condition, the same sounds were presented separately to the left and to the right ear (stereo) with intensity increasing in one ear while decreasing simultaneously in the other ear, creating the vivid perception of a sound moving from one ear to the other in the azimuth. All participants reported a strong sensation of motion. In the static condition, 1 s and 1.8 s pink noise sounds (mono) of constant intensity were presented. A 25 ms ascending/descending ramp was applied at the beginning/end of the static sounds. In order to ensure equal global acoustic energy across conditions despite the application of a ramp in the static condition, the static sounds were normalized based on the mean Root Mean Square (RMS) of the sounds from the motion conditions. Examples of the auditory stimuli used in the present study are provided in the Supplementary Material.

A block design was implemented in a single run consisting of 30 consecutive blocks (10 repetitions/category) separated by rest periods of 9 s. The three categories repeated consecutively with no randomization (i.e. lateral–in-depth–static). Each block included 18 consecutive auditory stimuli (no ISI) (Fig. 1A). Stimuli within the motion blocks always

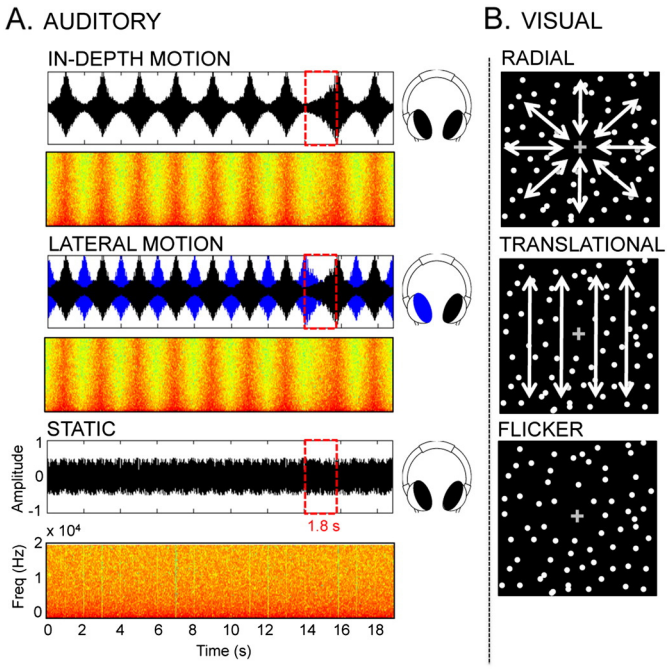

Fig. 1. Illustration of the stimuli used in (A) the auditory and (B) the visual experiment. (A) Sound properties of a representative block from the in-depth motion (looming/receding), lateral motion (leftward/rightward) and static (no motion) condition. Graphs represent the amplitude of a block as a function of time (waveform) and the spectrum of frequencies as a function of time (frequency spectrum). Red dashed lines indicate the occurrence of a 1.8 s target sound. The standard sounds were 1 s duration. The sounds delivered to each ear were in-phase in the in-depth motion condition and in the static condition (black waveforms represent the sound delivered to the two ears), and out-of-phase in the lateral motion condition (black/blue waveforms represent the sounds delivered to the right/left ear). For the lateral motion block, frequency spectrum is represented only for the sounds delivered to the right ear. The waveform for that sound is represented in black. The auditory blocks illustrated in this figure are also provided in the Supplementary Material. (B) Stimuli in the visual experiment were generated from random-dot patterns consisting of 3 different categories in analogy to the auditory experiment: radial motion (approaching/receding), translational (upward/downward) motion, and (3) flicker (no motion).

alternated between the two opposite directions (approaching and receding in the in-depth condition, left-to-right and right-to-left in the lateral motion condition). The task consisted of detecting longer (1.8 s) sounds by pressing the response button with the index finger of the right hand. Subjects were asked to respond as accurately as possible. Response speed was not emphasized. Within each category, there were 4 blocks with one target (18.8 s duration), 4 blocks with 2 targets (19.6 s duration) and 2 blocks with 3 targets (20.4 s duration). The whole run contained a total of 18 targets/category.

2.2.2. Visual experiment

Visual stimuli were generated from random-dot patterns consisting of 3 different categories in analogy to the auditory experiment: (1) radial motion, (2) translational (vertical) motion, and (3) flicker (no motion) (Fig. 1B). Vertical rather than lateral motion was used in the translational condition in order to minimize the generation of saccades (Morrone et al., 2000). Conversely, in the auditory experiment, laterally moving sounds were used because the use of headphones challenges the perception of vertically moving sounds. Moreover, previous work has shown that processing of vertically vs. laterally moving sounds (over static sounds) is supported by similar neural substrates (Pavani et al., 2002). Details of the stimuli used in the visual experiment are presented in the Supplementary Material.

A block design was implemented in a single run consisting of 30 consecutive blocks (10 repetitions/category) of 21 s duration each, separated by rest periods of 9 s. Each block consisted of 14 stimuli presented consecutively with no ISI. Stimuli within motion blocks always alternated between the two opposite directions (expanding and contracting in the radial condition, moving upward and downward in the vertical motion condition). In the radial condition, stimuli were designed to simulate in-depth motion (toward or away from the viewer). The task consisted of detecting a 500 ms (30 frames) color change (from white to gray) in the central fixation cross by pressing the response button with the index finger of the right hand. Subjects were asked to respond as accurately as possible. Response speed was not emphasized. For each category, there were 5 blocks with one target and 5 blocks with 2 targets. The whole run contained a total of 15 targets/category.

2.3. Behavioral analysis

Performance in the auditory run was analyzed by submitting accuracy scores (hits minus false alarms) to a 2 (between-subjects factor group) × 3 (within-subjects factor condition) repeated measures ANOVA. In the sighted group, a repeated measures ANOVA (3 within-subjects factor condition) was performed on accuracy scores in the visual experiment. A Greenhouse–Geisser correction was applied to the degrees of freedom and significance levels whenever an assumption of sphericity was violated.

2.4. fMRI data acquisition and analyses

2.4.1. Acquisition

Functional MRI-series were acquired using a 3-T TRIO TIM system (Siemens, Erlangen, Germany), equipped with a 12-channel head coil. Multislice T2*-weighted fMRI images were obtained with a gradient echo-planar sequence using axial slice orientation (TR = 2200 ms, TE = 30 ms, FA = 90°, 35 transverse slices, 3.2 mm slice thickness, 0.8 mm inter-slice gap, FoV = 192 × 192 mm^2, matrix size = 64 × 64 × 35, voxel size = 3 × 3 × 3.2 mm^3). Slices were sequentially acquired along the z-axis in feet-to-head direction. The 4 initial scans were discarded to allow for steady state magnetization. Participants' head was immobilized with the use of foam pads that applied pressure onto the headphones. A structural T1-weigthed 3D MP-RAGE sequence (voxel size = 1 × 1 × 1.2 mm^3; matrix size = 240 × 256; TR = 2300 ms, TE = 2.91 ms, TI = 900 ms, FoV = 256; 160 slices) was also acquired for all participants.

2.4.2. Univariate analyses

Functional volumes from the auditory and the visual experiments were pre-processed and analyzed separately using SPM8 (Welcome Department of Imaging Neuroscience, London), implemented in MATLAB (MathWorks).

Pre-processing included slice timing correction of the functional time series, realignment of functional time series, co-registration of functional and anatomical data, creation of an anatomical template using DARTEL (a template including participants from both groups in the auditory experiment, and a template including sighted participants only in the visual experiment) (Ashburner, 2007), spatial normalization of anatomical and functional data to the template, and spatial smoothing (Gaussian kernel, 8 mm full-width at half-maximum, FWHM). The creation of a study-specific template using DARTEL was performed to reduce deformation errors that are more likely to arise when registering single subject images to an unusually shaped template (Ashburner, 2007). This is particularly relevant when comparing early blind and sighted subjects as previous work has demonstrated significant structural differences in early blind subjects, particularly within the occipital cortex (Noppeney et al., 2005; Pan et al., 2007; Jiang et al., 2009; Park et al., 2009).

Following pre-processing steps, the analysis of fMRI data, based on a mixed effects model, was conducted in two serial steps accounting respectively for fixed and random effects. For each subject, changes in brain regional responses were estimated through a general linear model including the responses to the 3 experimental conditions (in-

depth motion, lateral motion and static conditions in the auditory experiment; radial, translational and flicker in the visual experiment). These regressors consisted of a boxcar function convolved with the canonical hemodynamic response function. Movement parameters derived from realignment of the functional volumes (translations in x, y and z directions and rotations around x, y and z axes) and a constant vector were also included as covariates of no interest. High-pass filtering was implemented in the design matrix using a cut-off period of 128 s to remove slow drifts from the time series. Serial correlations in fMRI signal were estimated using an autoregressive (order 1) plus white noise model and a restricted maximum likelihood (ReML) algorithm.

In the auditory experiment, linear contrasts tested the main effect of each condition ([in-depth], [lateral], [static]), the main effect of general auditory processing ([in-depth + lateral + static]), the main effect of motion processing ([in-depth + lateral > static]), the main effect of in-depth motion processing ([in-depth > lateral]), and the main effect of lateral motion processing ([lateral > in-depth]). Similarly, in the visual experiment, linear contrasts tested the main effect of each condition ([radial], [translational], [flicker]), the main effects of motion processing ([radial + translational > flicker]), the main effect of radial motion processing ([radial > translational]) and the main effect of translational processing ([translational > radial]). These linear contrasts generated statistical parametric maps [SPM(T)]. The resulting contrast images were then further spatially smoothed (Gaussian kernel 6 mm FWHM) and entered in a second-level analysis, corresponding to a random effects model, accounting for inter-subject variance. In the auditory experiment, one-sample t-tests were run on each group separately. Analyses characterized the main effect of each condition ([in-depth], [lateral], [static]), the main effect of general auditory processing ([in-depth + lateral + static]), the main effect of motion processing ([in-depth + lateral > static]), the main effect of in-depth motion processing ([in-depth > lateral]) and the main effect of lateral motion processing ([lateral > in-depth]). Two-sample t-tests were then performed to compare these effects between groups ([sighted > blind], [blind > sighted]). In the visual experiment, one-sample t-tests were run on the sighted sample. Analyses characterized the main effect of each condition ([radial], [translational], [flicker]), the main effects of motion processing ([radial + translational > flicker]), the main effect of radial motion processing [radial > translational] and the main effect of translational processing ([translational > radial]).

2.4.3. Functional connectivity analyses

Psychophysiological interaction (PPI) analyses (Gitelman et al., 2003) identify voxels in which activity is more related to activity in a seed region of interest (seed ROI) in a given psychological context. In the present study, PPI analyses were performed in order to identify brain regions that were more functionally coupled with the right planum temporale while processing moving vs. static auditory information. We selected this region as a seed because it showed identical auditory motion selectivity ([in-depth + lateral > static]) in both groups. In each individual, time-series of activity (first eigenvariate) from the seed area were extracted from the local maxima detected within 15 mm of the peak identified in the corresponding group, based on the [in-depth + lateral > static] contrast (in the blind and the sighted group, respectively, [66 – 34 16] and [64 – 34 14], see Fig. 2A and Table 1). New linear models were generated at the individual level, using three regressors. One regressor represented the condition (i.e. in-depth + lateral > static). The second regressor was the activity extracted in the seed area. The third regressor represented the interaction of interest between the first (psychological) and the second (physiological) regressors. To build this regressor, the underlying neuronal activity was first estimated by a parametric empirical Bayes formulation, combined with the psychological factor and subsequently convolved with the hemodynamic response function (Gitelman et al., 2003). The design matrix also included movement parameters as a regressor of no interest. A significant PPI indicated a change in the regression coefficients between any reported brain area and the seed area, related to the experimental condition ([in-depth + lateral > static]). The voxels identified in this analysis show a pattern of activity correlated with the seed region. Individual summary statistic images obtained at the first level (fixed effects) analysis were spatially smoothed (6-mm FWHM Gaussian kernel) and entered in a second-level (random effects) analysis using one-sample t-test. Two-sample t-tests were then performed to identify changes in functional connectivity between groups ([sighted > blind], [blind > sighted]).

2.4.4. Multivariate pattern analyses

Preprocessing steps were identical to the steps performed for univariate analyses, except for functional time series that were smoothed with a Gaussian kernel of 2 mm (FWHM). Multivariate pattern analyses were performed in CoSMoMVPA (http://www.cosmomvpa.org/; Oosterhof et al., 2016) implemented in Matlab (Mathworks). A general linear model was implemented in SPM8 separately for the auditory and visual experiments, where each block was defined as a regressor of interest. A beta map was calculated for each block separately. The beta maps were normalized (de-meaning) at each sphere within the searchlight and used as the input for the MVPA analysis. A single multi-class linear support vector machine (SVM) classifier with a linear kernel with a fixed regularization parameter of $C = 1$ was trained and tested for each participant separately within each group.

In the visual experiment, a three-class classifier was trained and tested to discriminate between the 3 visual conditions (radial motion, translational motion and flickering dots). In the auditory experiment, a three-class classifier was trained and tested to discriminate between the response patterns of the 3 auditory conditions (in-depth motion, lateral motion and static sounds). A separate binary auditory classifier was trained and tested to discriminate between the response patterns of the 2 auditory motion conditions (in-depth motion vs. lateral motion). The latter aimed at detecting regions that not only distinguished sound motion versus static information but also coded for different motion planes. A "leave-one block out" cross-validation scheme was implemented for each participant. The cross-validation procedure was carried out by dividing the dataset into two sub-sets (training and testing data). The classifier was trained on all blocks minus one ($n = 9$) from each condition and tested on the left out blocks. To evaluate the performance of the classifier and its generalization across all the data, the previous step was repeated 10 times (N-fold cross-validation where N is equivalent to the number of blocks in each condition) where in each fold a different block was used as the testing data and the classifier was trained on the other blocks. A single classification accuracy was obtained for each subject in each voxel by averaging the obtained accuracies from each cross-validation fold. The design was purposely implemented by having the 3 conditions repeated consecutively with no randomization (i.e. lateral–in-depth–static). Each block condition was therefore 2 blocks away from the block with the same condition (~66 and ~69 s between the end of a block from a given condition and the beginning of the next block from the same condition in the auditory and the visual experiment, respectively). This gives enough separation for independence between training and testing blocks of the same condition therefore avoiding inflated decoding accuracy due to temporal dependencies in fMRI time series.

Multivoxel pattern analyses were first performed in a hypothesis-free manner by scanning the entire brain for auditory-motion sensitive areas using a spherical-searchlight approach (Kriegeskorte et al., 2006). We defined a sphere of 3 voxels radius (117 voxels) that moved across the entire brain, where each voxel became the center of the searchlight sphere in turn, and multivariate patterns were analyzed locally within the searchlight sphere at each location (Kriegeskorte et al., 2006). These analyses led to classification accuracy at each voxel for each participant and the resulting whole brain accuracy maps were then further spatially smoothed (Gaussian kernel 6 mm FWHM). To perform the group level analysis in SPM8, a chance level accuracy map (33.33%

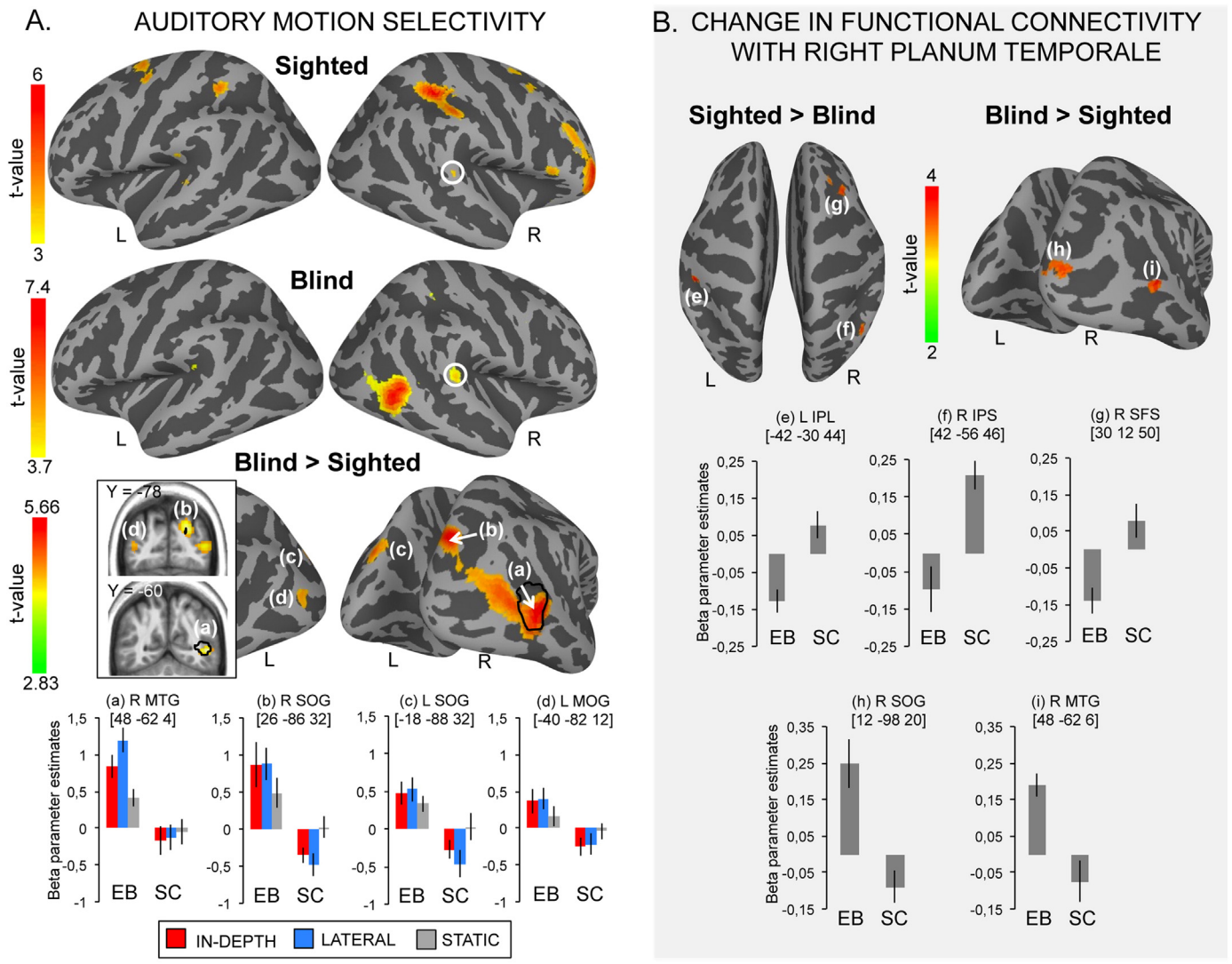

Fig. 2. Results of the whole brain univariate analyses. (A) Auditory motion selective activity resulting from the contrast [in-depth + lateral > static], in the sighted, the blind group and in the between group comparison (blind > sighted) (displayed at $p_{uncorr} < 0.001$). Outlined in black are hMT+/V5 and V3A as localized in the sighted in vision (displayed at $p_{uncorr} < 0.001$). For illustration, mean activity estimates (arbitrary units ± SEM) associated with the perception of in-depth motion (red), lateral motion (blue) and static sounds (gray) are plotted for blind and sighted at significant peaks. (B) Regions showing increased task-related [in-depth + lateral > static] connectivity with the right planum temporale seed area (circled in white in the left part of the figure) in the sighted compared to the blind and in the blind compared to the sighted (displayed at $p_{uncorr} < 0.001$). For illustration, mean strength of connectivity (arbitrary units ± SEM) are plotted for blind and sighted at significant peaks. Color bars represent t-values. L = left hemisphere, R = right hemisphere. See Tables 1, 2 and 4 for a list of brain regions depicted in this figure. See also Supplementary Fig. 2.

and 50% for the multi-class and binary decoding, respectively) was subtracted from each participant's classification accuracy map. The resulting contrast maps were then imported to SPM8 and entered in a second-level analysis, corresponding to a random effects model, accounting for inter-subject variance (Klein and Zatorre, 2014). One sample t-tests testing for above chance classification accuracy were run on each group separately in the auditory experiment, and in the sighted group only in the visual experiment. In the auditory experiment, two sample t-tests were then performed to identify group effects ([sighted > blind], [blind > sighted]).

2.4.5. Statistical inferences

The resulting set of voxel values for each contrast in the univariate, multivariate searchlight and psychophysiological interaction analyses constituted a map of the t statistic [SPM(T)] that was thresholded at $p < 0.001$ (uncorrected for multiple comparisons) in combination with a cluster threshold of 20 contiguous voxels, and 5 voxels in specific structures of interest (i.e. intraparietal sulci, planum temporale, hMT+/V5, V3A). Statistical inferences were performed at the voxel level using a threshold of $p < 0.05$ after correction for multiple comparisons (Family Wise Error method) over either the entire brain volume, or over small spherical volumes (15-mm radius) located in structures of interest reported by published work on visual motion and auditory motion/spatial processing. Coordinates (in MNI space) used for small volume correction are reported in the corresponding table legends. In the tables reporting findings from the auditory experiment (Tables 1–3), correction over small spherical volumes in bilateral hMT+/V5 and right V3A were performed on the coordinates of these areas as independently localized in vision based on the contrast [radial + translational > flicker] (see Table 4). Significant clusters were anatomically labeled using brain atlases (Petrides, 2012).

2.4.6. Regions of interest analyses

Previous studies have shown that group averaged responses for the localization of visual area hMT+/V5 can produce spurious overlapping responses to visual, tactile (Jiang et al., 2015) and auditory motion

Table 1
Results of the univariate analyses for the main effect of auditory motion processing [in-depth + lateral > static] in the blind and the sighted. Coordinates reported in this table are significant ($p < 0.05$ FWE) after correction over small spherical volumes (SVC) or over (*) the whole brain. Coordinates used for correction over small spherical volumes are as follows (x, y, z, in MNI space): left superior temporal gyrus [−54 −36 14] (Pavani et al., 2002); right superior temporal gyrus [64 −26 10] (Pavani et al., 2002); left superior parietal lobule [−30 −54 64] (Pavani et al., 2002); right intraparietal sulcus [36 −40 40] (Collignon et al., 2011); right superior frontal sulcus [32 0 48] (Collignon et al., 2011); left precentral gyrus [−40 −6 60] (Pavani et al., 2002); right precentral gyrus [46 4 36] (Pavani et al., 2002); right middle occipital gyrus [48 −76 6] (Collignon et al., 2011); left middle temporal gyrus (hMT+/V5) [−42 −64 4] (present study); right middle temporal gyrus (hMT+/V5) [42 −60 4] (present study); left superior occipital gyrus [−20 −80 30] (Collignon et al., 2011); right superior occipital gyrus (V3A) [22 −80 28] (present study). K represents the number of voxels when displayed at p(unc) < 0.001. L: left, R: right, G: gyrus, S: sulcus.

Area	k	x (mm)	y (mm)	z (mm)	Z	p
SIGHTED [IN-DEPTH + LATERAL > STATIC]						
R intraparietal S	528	34	−40	46	4.74	0.019*
R middle frontal G (anterior)	1423	34	44	8	4.56	0.037*
R inferior precentral S		60	16	26	3.63	0.011
L superior precentral S	337	−26	−6	56	3.72	0.009
L precentral G		−34	−6	54	3.72	0.008
L intraparietal S	80	−36	−48	52	3.30	0.028
L planum temporale	61	−52	−28	8	3.44	0.02
R superior frontal S	147	28	6	54	3.34	0.026
R middle/superior frontal G		34	2	60	3.29	0.029
R planum temporale	8	64	−34	14	3.22	0.035
BLIND [IN-DEPTH + LATERAL > STATIC]						
R middle temporal G	562	48	−60	4	5.29	0.002*
R planum temporale	243	66	−34	16	3.81	0.006
R precentral G	72	54	4	48	3.43	0.02
R precentral G		58	8	38	3.28	0.03
L rolandic operculum	37	−42	−36	24	3.36	0.024
R superior occipital G	27	26	−86	34	3.14	0.044
R superior occipital G		26	−80	34	3.13	0.045
R intraparietal S	7	32	−40	48	3.22	0.036
L intraparietal S	6	−32	−46	50	3.17	0.042
BLIND > SIGHTED [IN-DEPTH + LATERAL > STATIC]						
R middle temporal G	1678	48	−62	4	4.53	0.043*
R superior occipital G		26	−86	32	4.48	0.001
R lateral occipital sulcus/middle occipital G		44	−76	10	3.77	0.007
L superior occipital G	176	−18	−88	32	3.79	0.007
L middle occipital G	62	−40	−78	8	3.20	0.039

Table 2
Results of the functional connectivity (PPI) analyses performed on the main effect of auditory motion processing [in-depth + lateral > static] in the blind and the sighted using the right planum temporale as a seed. Coordinates reported in this table are significant ($p < 0.05$ FWE) after correction over small spherical volumes (SVC). Coordinates used for correction over small spherical volumes are as follows (x, y, z, in MNI space): left superior temporal gyrus [−54 −36 14] (Pavani et al., 2002); left inferior parietal lobule [−48 −30 44] (Griffiths et al., 2000); right inferior parietal lobule [42 −50 32] (Weeks et al., 2000); right superior frontal sulcus [32 0 48] (Collignon et al., 2011); left supplementary motor area [−2 12 52] (Lewis et al., 2000); left precentral gyrus [−40 −6 60] (Pavani et al., 2002); right precentral gyrus [46 4 36] (Pavani et al., 2002); right middle temporal gyrus (hMT+/V5) [42 −60 4] (present study); left cuneus [0 −90 22] (Bedny et al., 2010). K represents the number of voxels when displayed at p(unc) < 0.001. L: left, R: right, G: gyrus, S: sulcus.

Area	k	x (mm)	y (mm)	z (mm)	Z	p
PPI SIGHTED [IN-DEPTH + LATERAL > STATIC]						
R supplementary motor area	309	2	8	56	3.85	0.006
R precentral/middle frontal G	124	40	2	56	3.84	0.007
L rolandic operculum	60	−46	−40	24	3.73	0.009
R inferior frontal G (opercular part)	42	44	12	26	3.36	0.027
L precentral G	46	−44	−4	52	3.32	0.03
PPI BLIND [IN-DEPTH + LATERAL > STATIC]						
L cuneus/superior occipital G	503	−4	102	18	4.22	0.002
R cuneus/superior occipital G		10	−98	22	4.19	0.002
R middle temporal G	28	48	−62	4	3.64	0.012
R precentral G	29	50	0	48	3.43	0.023
PPI SIGHTED > BLIND [IN-DEPTH + LATERAL > STATIC]						
L inferior postcentral S/inferior parietal lobule	24	−42	−30	44	3.47	0.02
R intraparietal S	33	42	−56	46	3.33	0.03
R superior frontal S	44	30	12	50	3.31	0.031
PPI BLIND > SIGHTED [IN-DEPTH + LATERAL > STATIC]						
R cuneus/superior occipital G	161	12	−98	20	3.52	0.017
R middle temporal G	16	48	−62	6	3.39	0.025

(Saenz et al., 2008). These spurious overlapping responses are thought to arise because the location of visual area hMT+/V5 varies widely across individuals (Dumoulin et al., 2000; Huk et al., 2002). To further investigate the presence of auditory motion information in area hMT+/V5 of the sighted, auditory decoding analyses (three-class and binary) were conducted within hMT+/V5 as independently localized in vision based on the contrast [radial + translational > static]. These analyses were computed within both group-defined and individually-defined coordinates of hMT+/V5.

A sphere of 6-mm radius (117 voxels) was created around the peak of the group coordinate, and of each single subject coordinate of left and right hMT+/V5, thus resulting in 4 ROIs. For illustration purposes, beta parameter estimates resulting from the univariate analyses were extracted for the 3 auditory and the 3 visual conditions in these ROIs (Fig. 5A). Multi-class and binary multivariate pattern analyses were conducted (as described in Section 2.4.4) within these ROIs in the auditory experiment only (Fig. 5B).

The resulting multi-class and binary classification accuracy was analyzed separately as follows. First, one-sided one-sample t-tests tested for above chance level decoding accuracy (i.e. 33.33% and 50% for the multi-class and binary classification, respectively) in each ROI (Bonferroni correction for multiple comparisons). Second, a 2 × 2 repeated measure ANOVAs tested the effect of coordinate (group-defined, individually-defined) and hemisphere (left, right hMT+/V5) in these ROIs. A Greenhouse–Geisser correction was applied to the degrees of freedom and significance levels whenever an assumption of sphericity was violated.

3. Results

3.1. Behavioral results

3.1.1. Auditory experiment

The main effect of group was not significant, indicating that overall target detection accuracy (hits – false alarms) did not differ between the blind (mean ± SD = 94.7% ± 4.9%) and the sighted groups (mean ± SD = 90.03% ± 8.54%). However, there was a significant main effect of condition ($F_{2,52} = 11.107$; $p = 0.001$). Two-tailed paired-sample t-tests, collapsed across participants, indicated overall lower detection accuracy in the in-depth motion condition (mean ± SD = 86.9% ± 13.37%) compared to the lateral motion (mean ± SD = 94.25% ± 8.07%; $t_{27} = -2.908$, $p = 0.007$) and to the static conditions (mean ± SD = 96.43% ± 6.45%; $t_{27} = -3.905$, $p = 0.001$). The interaction was not significant ($p > 0.2$).

3.1.2. Visual experiment

Target detection accuracy was high in all conditions (radial: mean ± SD = 93.85% ± 5.06%; translational: mean ± SD = 92.82% ± 9.6%; flicker: mean ± SD = 91.8% ± 9.87%). The main effect of condition was not significant, indicating that detection accuracy was equivalent across conditions.

3.2. fMRI results — univariate analyses

In line with previous work (Pavani et al., 2002; Seifritz et al., 2002; Warren et al., 2002), sighted subjects showed auditory motion selective activity (compared to static) in a fronto-temporo-parietal network

Table 3
Results of the three-class and binary multivariate searchlight analyses obtained in the auditory experiment in the blind and the sighted. Coordinates reported in this table are significant ($p < 0.05$ FWE) after correction over small spherical volumes (SVC) or over (*) the whole brain. Z and p-values are relative to chance performance (33.33% and 50% for multi-class and binary classification, respectively). For binary classification (right hand), coordinates marginally significant are reported in italic and underlined.
Coordinates used for correction over small spherical volumes are as follows (x, y, z, in MNI space): left superior temporal gyrus [−54 −36 14] (Pavani et al., 2002); right superior temporal gyrus [64 −26 10] (Pavani et al., 2002); left Heschl's gyrus [−40 −28 8] (Hart et al., 2004); right Heschl's gyrus [52 −16 8 8] (Hart et al., 2004); left inferior parietal lobule [−48 −30 44] (Griffiths et al., 2000); right inferior parietal lobule [42 −50 32] (Weeks et al., 2000); left superior parietal lobule [−30 −54 64] (Pavani et al., 2002); right superior parietal lobule [26 −62 62] (Pavani et al., 2002); right intraparietal sulcus [36 −40 40] (Collignon et al., 2011); right superior frontal sulcus [32 0 48] (Collignon et al., 2011); left supplementary motor area [−2 12 52] (Lewis et al., 2000); left precentral gyrus [−40 −6 60] (Pavani et al., 2002); right precentral gyrus [46 4 36] (Pavani et al., 2002); left middle temporal gyrus (hMT+/V5) [−42 −64 4] (present study); right middle temporal gyrus (hMT+/V5) [42 −60 4] (present study); left superior occipital gyrus [−20 −80 30] (Collignon et al., 2011); right superior occipital gyrus (V3A) [22 −80 28] (present study); left cuneus [0 −90 22] (Bedny et al., 2010); right precuneus [4 −58 62] (Griffiths et al., 2000). For each SVC, we only report the highest peak coordinate located within a given structure of interest in the multi-class analyses, and the corresponding coordinate in the binary class analyses. K represents the number of voxels when displayed at p(unc) < 0.001. L: left, R: right, G: gyrus, S: sulcus.

Area	k	x (mm)	y (mm)	z (mm)	Z	p	k	x (mm)	y (mm)	z (mm)	Z	p
Multi-class decoding							Binary decoding					
SIGHTED							*SIGHTED*					
R sulcus of Heschl	3610	60	−10	6	6.25	<0.001*	5024	60	−12	4	6.74	<0.001*
R planum temporale		58	−26	8	5.75	<0.001*		48	−24	12	5.09	0.017*
R planum temporale		68	−20	4	5.59	0.001*						
R middle temporal G		48	−56	12	3.98	0.007		50	−62	16	4.40	0.015
L sulcus of Heschl	2956	−52	−22	6	5.95	<0.001*	3875	−52	−18	6	5.64	0.003*
L planum temporale		−66	−34	12	5.95	<0.001*		−64	−34	8	5.79	0.002*
L planum temporale		−42	−32	12	5.02	0.013*		−56	−8	2	5.08	0.017*
L anterior occipital S	123	−50	−68	2	3.81	0.012		−48	−62	8	4.35	0.002
L middle temporal G	85	−48	−62	16	3.44	0.036		−40	−74	4	3.60	0.027
R supramarginal G/inferior parietal Lobule	165	40	−34	40	3.91	0.009	567	38	−38	36	3.58	0.029
R inferior parietal lobule		38	−40	40	3.53	0.027		40	−38	36	3.45	0.041
R precuneus	335	2	−54	58	3.38	0.042	169	−4	−44	60	3.66	0.023
R middle/superior occipital G	502	32	−90	24	4.21	0.003	88	34	−76	36	4.29	0.003
R superior occipital G		20	−84	42	3.66	0.019						
L cuneus	199	−6	−90	24	3.75	0.014	–	–	–	–	–	–
L precentral G	308	−42	−6	50	3.71	0.016	(3875)	−44	−6	46	3.64	0.024
R precentral G	128	56	0	44	3.87	0.01	(5024)	62	−6	30	5.20	0.015*
R precentral G		58	10	32	3.42	0.037	(5024)	58	10	30	4.18	0.004
R superior precentral S	20	28	−6	52	3.44	0.035	–	–	–	–	–	–
L supplementary motor area	85	0	2	58	3.81	0.012	27	6	18	52	3.48	0.038
L superior parietal lobule	243	−28	−54	50	3.75	0.014	279	−28	−54	50	3.71	0.02
L inferior parietal lobule		−52	−36	32	3.74	0.015		−58	−32	34	3.53	0.033
L superior occipital G	50	−30	−90	26	3.71	0.016	93	−24	−80	36	3.87	0.012
R postcentral G/superior parietal lobule	560	26	−48	60	4.27	0.002	(567)	32	−48	60	3.81	0.014
R superior parietal lobule		18	−62	62	4.18	0.003		22	−56	64	3.57	0.03
BLIND							*BLIND*					
R middle temporal G	4371	46	−58	10	5.76	<0.001*	4461	50	−64	16	5.27	0.006*
R middle temporal G		50	−48	10	5.44	0.002*		54	−42	8	4.98	0.021*
R planum temporale		54	−38	14]	4.79	0.034*		56	−36	16	4.33	0.002
R sulcus of Heschl		56	−12	4	3.90	0.009	124	56	−12	4	3.99	0.008
L anterior occipital S	2578	−52	−62	6	4.91	0.021*	2340	−50	−62	6	5.18	0.008*
L middle temporal G		−48	−64	16	4.73	0.043*		−46	−58	12	4.86	0.033*
L sulcus of Heschl/PT		−66	−36	14	4.41	0.001	160	−50	−34	16	4.16	0.005
L sulcus of Heschl		−54	−30	12	3.86	0.01						
R precuneus	3977	12	−50	62	4.81	0.033*	(446)	10	−48	60	4.25	0.003
L precuneus		−6	−46	58	4.64	0.04*	(446)	−6	−56	50	4.76	0.049*
R inferior parietal lobule		32	−40	54	4.30	0.01	(446)	32	−40	52	3.90	0.011
R superior parietal lobule		24	−48	60	4.30	0.002	(446)	36	−56	58	3.41	0.047
L IPS/superior parietal lobule		−38	−48	58	3.86	0.01	(234)	−32	64	54	3.58	0.029
R superior occipital G	301	22	−84	40	3.83	0.011	626	20	−88	32	4.17	0.004
L cuneus		−2	−76	24	3.40	0.039		*−2*	*−76*	*26*	*3.26*	*0.069*
L superior occipital G	135	−20	−80	32	4.09	0.005	(2340)	−24	−82	38	4.52	0.001
R superior occipital G	130	22	−84	40	3.83	0.011	(626)	20	−88	32	4.17	0.004
R superior precentral S	76	28	−4	50	4.01	0.006	*4*	*26*	*−4*	*52*	*3.20*	*0.081*
R precentral G	177	52	2	44	3.93	0.008	621	52	4	44	3.52	0.035
L precentral G	94	−42	−4	50	3.81	0.012		–	–	–	–	–
SIGHTED > BLIND							*SIGHTED > BLIND*					
R planum temporale	70	62	−10	6	3.79	0.013	298	60	−12	6	4.31	0.003
L sulcus of Heschl	49	−52	−22	6	3.52	0.028	*4*	*−50*	*−20*	*6*	*3.23*	*0.075*
L supramarginal gyrus		−58	−22	14	3.37	0.043	*6*	*−64*	*−32*	*6*	*3.17*	*0.087*
BLIND > SIGHTED							*BLIND > SIGHTED*					
R middle temporal gyrus	21	40	−60	6	3.37	0.043	*7*	*52*	*−70*	*0*	*3.19*	*0.08*

subtending the intraparietal sulci, the superior frontal/precentral gyri, the planum temporale bilaterally, and a large cluster encompassing the inferior and middle frontal gyrus in the right hemisphere (Figs. 2A, 3A, Table 1). In the blind group, auditory motion selective responses were also observed in the right planum temporale, and to a smaller extent, in the right precentral gyrus and bilateral intraparietal sulci. In this

Table 4
Results of the univariate analyses and three-class multivariate analyses obtained in the visual experiment in the sighted. Coordinates reported in this table are significant ($p < 0.05$ FWE) after correction over small spherical volumes (SVC) or over (*) the whole brain. Coordinates used for correction over small spherical volumes are as follows (x, y, z, in MNI space): left hMT+/V5 [−42 −68 −2] (Sunaert et al., 1999); right hMT+/V5 [42 −64 4] (Sunaert et al., 1999); right superior occipital gyrus [24 −80 26] (Sunaert et al., 1999). K represents the number of voxels when displayed at p(unc) < 0.001. L: left, R: right, G: gyrus, S: sulcus.

Area	k	x (mm)	y (mm)	z (mm)	Z	p
[RADIAL + TRANSLATIONAL > FLICKER]						
R middle temporal G (hMT+/V5)	351	42	−60	4	5.51	0.001*
L middle temporal G (hMT+/V5)	49	−34	−66	4	3.37	0.021
		−42	−64	4	3.23	0.03
R superior occipital G (V3A)	15	22	−80	28	3.24	0.029
MULTIVARIATE DECODING OF THE 3 VISUAL CONDITIONS						
L middle occipital G (hMT+/V5)	797	−44	−74	4	4.22	0.01
R middle temporal G (hMT+/V5)	171	44	−62	6	3.67	0.049

group, responses were additionally observed in the left rolandic operculum and in the right superior occipital gyrus. The strongest selectivity (resisting whole brain correction) was observed in a cluster located in the right posterior middle temporal gyrus (Figs. 2A, 3A, Table 1).

A two-sample t-test [blind > sighted] performed on the main effect of motion processing [in-depth + lateral > static] revealed bilateral activations with a right hemispheric dominance (Fig. 2A, Table 1, see also Supplementary Fig. 2). Activations were observed in the right posterior middle temporal gyrus extending into the right middle occipital gyrus, in the left middle occipital gyrus and in the superior occipital gyri bilaterally (Fig. 2, Table 1). Importantly, only two clusters within these regions were significantly *activated* in the blind: the right posterior middle temporal gyrus and the right superior occipital gyrus. Significant differences between the groups observed in the left hemisphere were thus mainly driven by significant deactivation in the sighted. The right posterior middle temporal gyrus (MNI coordinates [48 – 62 4]) and the right superior occipital gyrus (MNI coordinates [26 – 86 32]) selective for auditory motion in the blind group overlapped with visual areas hMT+/V5 and V3A localized in the sighted group in vision by means of the contrast [radial + translational >flicker] (MNI coordinates [42 – 60 4] and [22 – 80 28], respectively, outlined in black in Fig. 2A, Table 4). No significant responses to auditory motion were observed in the sighted group in functionally-defined hMT+/V5 (or elsewhere in the occipito-temporal "visual" cortex) even at a more lenient threshold of $p < 0.01$ uncorrected.

We further explored selective reorganization for specific types of auditory motion ([in-depth > lateral], [lateral > in-depth]). These results are presented in Supplementary material (Supplementary Fig. 3 and Supplementary Table 3).

3.3. fMRI results — functional connectivity analyses

We ran psychophysiological interactions (PPI) analyses (Gitelman et al., 2003) in order to further investigate the impact of early visual deprivation on the brain network supporting auditory motion processing. These analyses targeted the right planum temporale as the seed area for two reasons. First, the right planum temporale has been consistently identified as a crucial region for supporting auditory motion processing in the present and in previous studies (Pavani et al., 2002; Seifritz et al., 2002; Warren et al., 2002). Second, as this area was commonly responsive to moving relative to static sounds in both groups of participants in the present study (Fig. 2A, white circled), connectivity analyses performed using this region as a seed cannot be biased in favor of one or the other group.

In the sighted group, the right planum temporale showed increased task-related connectivity with the left rolandic operculum, the medial superior frontal gyri (supplementary motor area), the bilateral precentral gyri, and right middle and inferior frontal gyri (Table 2). In the blind group, the right planum temporale showed increased task-related connectivity with the right posterior middle temporal gyrus, the bilateral cuneus, and the right precentral gyrus (Table 2). Between group comparisons indicated that the right planum temporale showed increased task-related connectivity in the blind (compared to the sighted group) with the right posterior middle temporal gyrus and the right cuneus/superior occipital gyrus (identified in the univariate analyses, see Fig. 2B, Table 2). In contrast, the same area showed increased task-related connectivity in the sighted (compared to the blind group) in a fronto-parietal network including the right intraparietal sulcus, the left inferior parietal lobule, and the right superior frontal sulcus. As illustrated by the beta parameter estimates in Fig. 2B, all of these regions showed opposite effects of functional connectivity between the two groups.

3.4. fMRI results — searchlight multivariate pattern analyses

3.4.1. Auditory experiment

Multi-class whole brain searchlight analyses allowed the identification of brain regions that successfully classified the three auditory conditions above chance level (33.33%) in the sighted and the blind (Figs. 3B and 4A, Table 3).

In both groups, significant decoding accuracy was observed in large portions of the auditory cortex bilaterally, including the planum temporale and the lateral part of Heschl's gyrus (primary/secondary auditory cortex). These clusters extended posteriorly across the middle temporal gyri toward the superior temporal sulci bilaterally. Significant classification was also observed in the cuneus and precuneus, in bilateral superior occipital gyri, in bilateral intraparietal sulci extending to the superior parietal lobules, in the right inferior parietal lobule, in bilateral precentral gyri and in the right superior precentral sulcus.

Decoding accuracy resisting whole brain correction was confined to the bilateral auditory cortices (encompassing Heschl's gyrus bilaterally) in the sighted group, and to bilateral posterior middle temporal gyri, bilateral precuneus and right planum temporale in the blind (Figs. 3B, 4A, Table 3).

In both groups, although to a lesser extent in the sighted, posterior clusters partially overlapped with regions of the occipito-temporal cortex that successfully decoded the 3 visual conditions in the sighted (Fig. 3B). Two sample t-tests were performed in order to compare these effects between groups. In line with the whole brain univariate analyses (Fig. 2A), a cluster located in the right posterior middle temporal gyrus showed higher multi-class decoding accuracy in the blind relative to the sighted group (MNI coordinates [40 – 60 6], Fig. 4A, Table 3). The reverse comparison revealed two clusters in bilateral planum temporale extending to the supramarginal gyrus in the left hemisphere, that showed higher classification accuracy in the sighted relative to the blind group (Fig. 4A, Table 3).

Follow up searchlight analyses using a binary classifier (in-depth vs. lateral motion) provided similar findings (compare Fig. 4A and B; see Table 3), thus indicating that the regions identified in the multi-class analyses not only distinguish dynamic vs. static information but further contain information about different auditory motion planes.

3.4.2. Visual experiment

In the visual experiment, the whole brain searchlight analyses identified a large portion of the left middle occipital gyrus (including hMT+/V5) and a cluster in the right middle temporal gyrus (hMT+/V5) that successfully decoded the three visual conditions above chance level (one-sample t-test) (see orange color in Fig. 3B, Table 4).

3.5. Regions of interest analyses in individually localized hMT+/V5 in sighted subjects

To further investigate the presence of auditory motion information in area hMT+/V5 of the sighted, we conducted additional analyses in this area. hMT+/V5 regions of interest were defined both at the

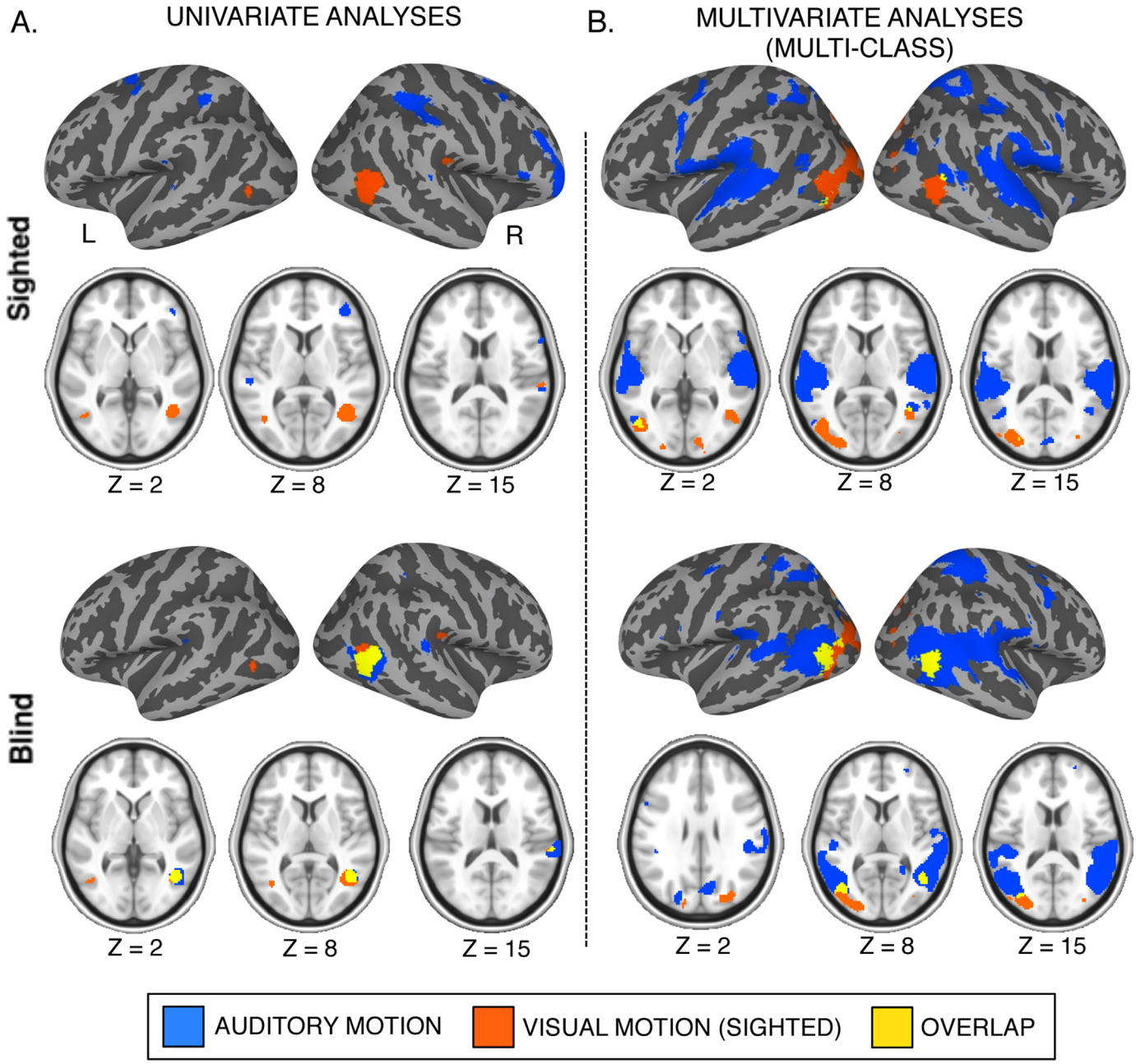

Fig. 3. Results of the whole brain univariate and multivariate analyses in the auditory (blue) and the visual (orange) experiments. (A) Auditory activations resulting from the contrast [in-depth + lateral > static] in the sighted and the blind and visual activations resulting from the contrast [radial + translational > flicker] in the sighted ($p_{uncorr} < 0.001$, $k > 20$). The overlap between auditory and visual responses is depicted in yellow. (B) Regions showing above chance level (33.33%) decoding of the 3 auditory conditions (in-depth motion, lateral motion, static) in the sighted and the blind and of the 3 visual conditions (radial motion, translational motion, flicker) in the sighted ($p_{uncorr} < 0.001$, $k > 20$). The overlap between auditory and visual decoding is depicted in yellow. L = left hemisphere, R = right hemisphere. See Tables 1, 3 and 4 for a list of brain regions depicted in this figure.

group and at the individual level based on the univariate contrast [radial + translational > static] in the visual experiment. These analyses were conducted in 12 sighted subjects for whom data was analyzed in both the auditory and the visual experiments (see Section 2.1). Right hMT+/V5 was identified in all 12 subjects, and left hMT+/V5 was identified in 11 out of 12 subjects. One subject for whom left hMT+/V5 could not be identified was removed from single coordinate analyses for left hMT+/V5.

Regarding univariate analyses, beta parameter estimates in these regions of interest were extracted for the 3 auditory and the 3 visual conditions. As expected, considering that location of visual area hMT+/V5 varies widely across individuals (Dumoulin et al., 2000; Huk et al., 2002), extracting visual responses within individually localized hMT+/V5 areas markedly increased the strength of the visual responses (Fig. 5A). In contrast, auditory responses were absent in these areas, whether these responses were extracted from group-averaged or individual coordinates of left and right hMT+/V5 (Fig. 5A). Thus, whether using group-averaged or individually localized hMT+/V5, univariate analyses indicate no evidence of auditory responses in this area in the sighted.

Multivariate pattern analyses in the auditory experiment were computed within left and right hMT+/V5 using both group-level and individual level coordinates. In these 4 ROIs, we tested the accuracy of classification of the 3 auditory conditions (multi-class decoding) and of the 2 auditory motion conditions only (binary decoding).

The 3 auditory conditions were classified significantly above chance level only in individually-defined left ($t_{10} = 2.35$, $p = 0.02$) and right

hMT+/V5 ($t_{11} = 3.1$, $p = 0.005$) while decoding accuracy did not differ from chance in group-defined ROIs ($p's > 0.1$). Above chance decoding accuracy resisted Bonferroni correction only in right individually-defined hMT+/V5 (Fig. 5B). There was a significant effect of coordinate ($F_{1, 10} = 9$, $p = 0.013$), indicating that multi-class decoding accuracy was overall higher when using individually-defined coordinates of

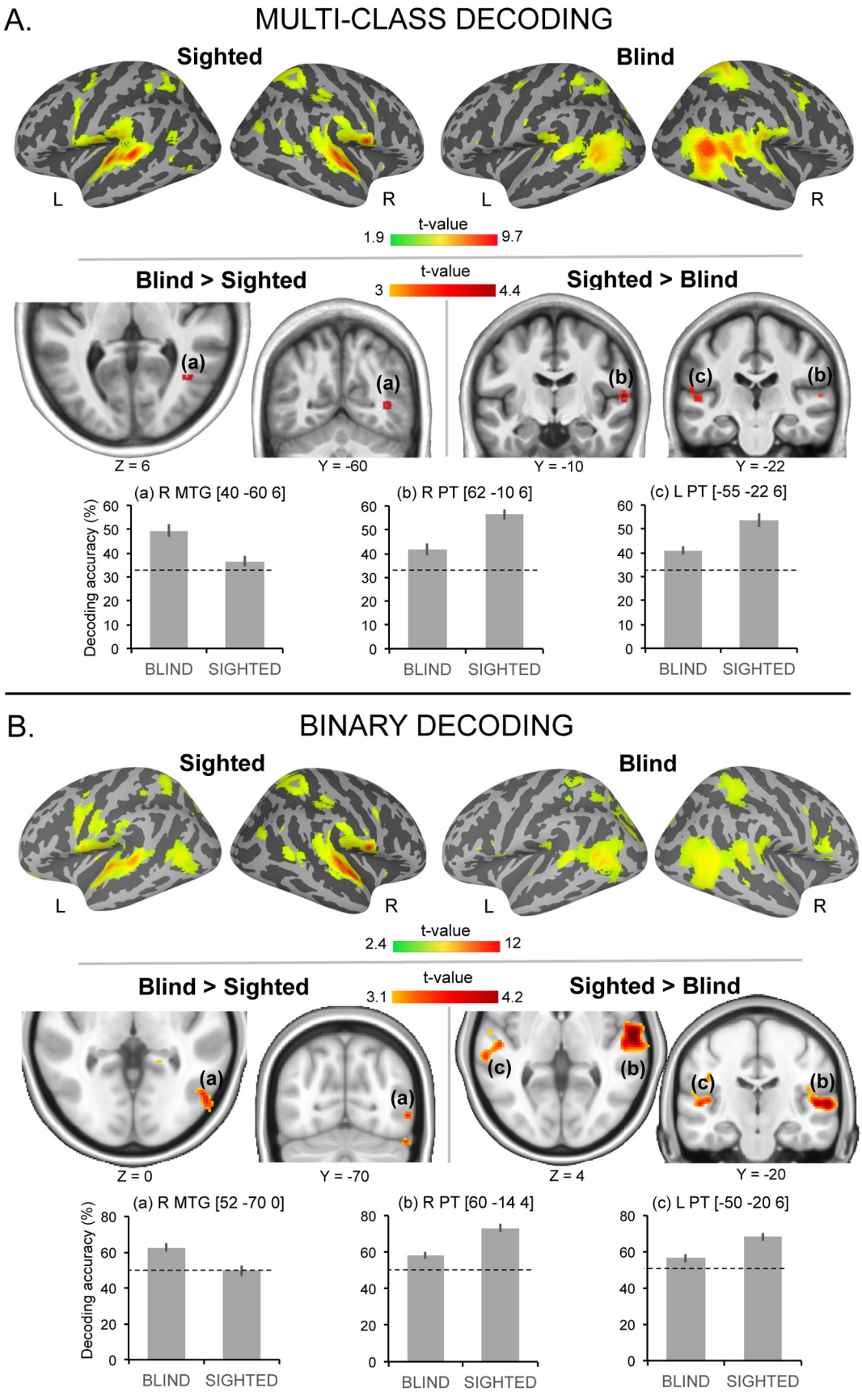

hMT+/V5 (mean ± SD collapsed across hemispheres = 44.9 ± 13.75) than group level coordinate of this area (mean ± SD collapsed across hemispheres = 35.27 ± 8.67). No other main effect of interaction were significant (p's > 0.4).

Binary classification of the 2 auditory motion conditions was significantly above chance level in both hemispheres when using individually-defined coordinates of hMT+/V5 (left hMT+/V5: t_{10} = 2.73, p = 0.01; right hMT+/V5: t_{11} = 2.75, p = 0.01), while it was only significant in the left hemisphere when using group-defined coordinates of this area (left hMT+/V5: t_{11} = 3.58, p = 0.002; right hMT+/V5: p = 0.09). There was no effect of coordinate (p > 0.2) or hemisphere (p > 0.3) on binary classification accuracy, and no interaction between these 2 factors (p > 0.15).

4. Discussion

The present study is the first to directly compare whole-brain uni- and multi-variate analyses using carefully controlled auditory motion stimuli in a rather large group of early blind individuals (n = 15).

4.1. Functional specialization for auditory motion processing in right hMT+/V5 and V3A of early blind subjects

In line with several studies investigating crossmodal reorganization associated with blindness, univariate analyses revealed substantial activity in the occipital cortex of the blind in response to general sound processing (Supplementary Fig. 1, Supplementary Table 2). A subset of these regions, more specifically the posterior middle temporal gyrus and superior occipital gyrus in the right hemisphere showed a preference for moving over static sounds selectively in the blind group (Fig. 2A). These regions overlapped with right hMT+/V5 and V3A (Watson et al., 1993; Tootell et al., 1995) localized visually in the sighted (Fig. 2A). In contrast to previous work (Poirier et al., 2006; Lewald and Getzmann, 2013), the findings in the present study revealed that auditory motion selectivity was confined to these right occipito-temporal regions. Our results therefore demonstrate that in the absence of visual input since birth, the right hMT+/V5 and V3A maintain their functional specialization toward the processing of dynamic information while redirecting their modality tuning toward sounds. These findings are consistent with the observation that nearby regions of the right dorsal stream preferentially respond to the spatial attributes of sounds in congenitally blind compared to sighted (Collignon et al., 2007, 2011) or late-blind individuals (Collignon et al., 2013). Together with the aforementioned studies and in line with the idea that visuo-spatial processing occurs predominantly in the right hemisphere in sighted individuals (Corbetta and Shulman, 2002), the present study supports a strong right hemispheric lateralization for auditory spatial processing in early blind subjects (Weeks et al., 2000; Collignon et al., 2011).

The findings of our study contrast with previous work suggesting that sounds with high motion content relative to sounds with low motion content are enhanced in blind subjects only in the left hMT+/V5 (Bedny et al., 2010). In the present study, despite higher auditory-driven activity in left middle occipital gyrus in the blind compared to the sighted group (Supplementary Fig. 1), only the right hMT+/V5 displayed significant auditory motion selective responses that were specific to the blind group (Fig. 2A, Supplementary Fig. 2). This apparent conflicting finding might be due to the different stimuli used in these studies. For instance, the high and low motion content stimuli in the study of Bedny et al. (2010) differed in terms of low-level properties and perceptual salience. Thus, any difference observed between conditions might be putatively associated with differences in the physical attributes of the sounds or in the level of arousal they generate, rather than to differences in motion content itself. In line with this assumption, it was recently shown that in congenitally blind humans hMT+/V5 displays a tonotopic mapping in response to pure tones of varying frequencies, suggesting that this region might be sensitive to early aspects of auditory processing in this population (Watkins et al., 2013). Using a whole-brain approach and moving vs. static stimuli differing solely in their motion content, the present study suggests that the selective increase in response to moving sounds in early blind subjects is specific to the right hMT+/V5 and V3A.

4.2. Crossmodal reorganization as a large-scale imbalance between sensory systems

Whole-brain searchlight MVPA analyses revealed an extended network of brain regions containing information about the 3 auditory conditions in both groups of subjects (Fig. 3B). These regions included the planum temporale and the posterior middle temporal gyri in the vicinity of hMT+/V5 in both groups. Results of the binary decoding were highly similar to the ones of the three-class decoding (Fig. 4A and B), thus demonstrating that these regions do not merely distinguish motion vs. static information but further contain information about different auditory motion planes.

Supporting the findings from the univariate analyses, the right posterior middle temporal gyrus (overlapping with the univariate definition of hMT+/V5) showed enhanced decoding accuracy in the blind relative to the sighted group (Fig. 4A). Importantly, classification accuracy in the planum temporale bilaterally was significantly higher in the sighted than in the blind group (Fig. 4A). Between-group comparisons using binary decoding (in-depth vs. lateral motion) confirmed these findings although with more marginal effects for the right posterior middle temporal gyrus (blind > sighted) and the left planum temporale (sighted > blind) (see Fig. 4B).

Reduced univariate activity in the auditory cortices was previously reported in early blind subjects during passive listening of sounds compared to silence (Gougoux et al., 2009; Stevens and Weaver, 2009; Watkins et al., 2013). A recent study using multivariate pattern analyses in regions of interest showed that the direction of moving sounds was accurately classified within the right planum temporale but not within hMT+/V5 in sighted subjects, whereas the reverse pattern was found in early blind subjects (Jiang et al., 2014). Likewise, in the present study, classification in the sighted compared to the blind was significantly higher in auditory regions and significantly reduced in right hMT+/V5. In contrast to findings reported by Jiang et al. (2014) however, we found reliable classification of motion-related information in both the planum temporale and hMT+/V5 in both early blind and sighted subjects. These findings suggest that following early visual deprivation, at least a portion of the computational resources dedicated to auditory motion processing and typically located in the planum temporale is redirected to the deafferented "visual" cortex. In other words, brain reorganization following early visual deprivation appears to be characterized by a large-scale reallocation of computational resources that are typically supported by the auditory cortex. This

Fig. 4. Results of the whole brain searchlight multivariate pattern analyses in the auditory experiment. (A) Multi-class decoding (in-depth motion, lateral motion, static): The top panel depicts regions showing above chance level (33.33%) decoding in the sighted and the blind group (p_{uncorr} < 0.001, k > 20). The bottom panel depicts regions showing significantly higher decoding accuracy in the blind compared to the sighted group and in the sighted compared to blind group (p_{uncorr} < 0.001, k > 20). For illustration, mean decoding accuracy (± SEM) of the 3 auditory conditions (in-depth motion, lateral motion, and static) is plotted for blind and sighted in 3 significant voxels (a, b and c). (B) Binary decoding (in-depth vs. lateral motion): The top panel depicts regions showing above chance level (50%) decoding in the sighted and the blind group (p_{uncorr} < 0.001, k > 20). The bottom panel depicts regions showing significantly higher decoding accuracy in the blind compared to the sighted group and in the sighted compared to blind group (p_{uncorr} < 0.005, k > 20). For illustration, mean decoding accuracy (± SEM) of the 2 auditory conditions (in-depth motion and lateral motion) is plotted for blind and sighted in 3 significant voxels (a, b and c). Color bars represent t-values relative to chance. L = left hemisphere, R = right hemisphere. Dotted lines represent chance level. See Table 3 for a list of brain regions depicted in this figure.

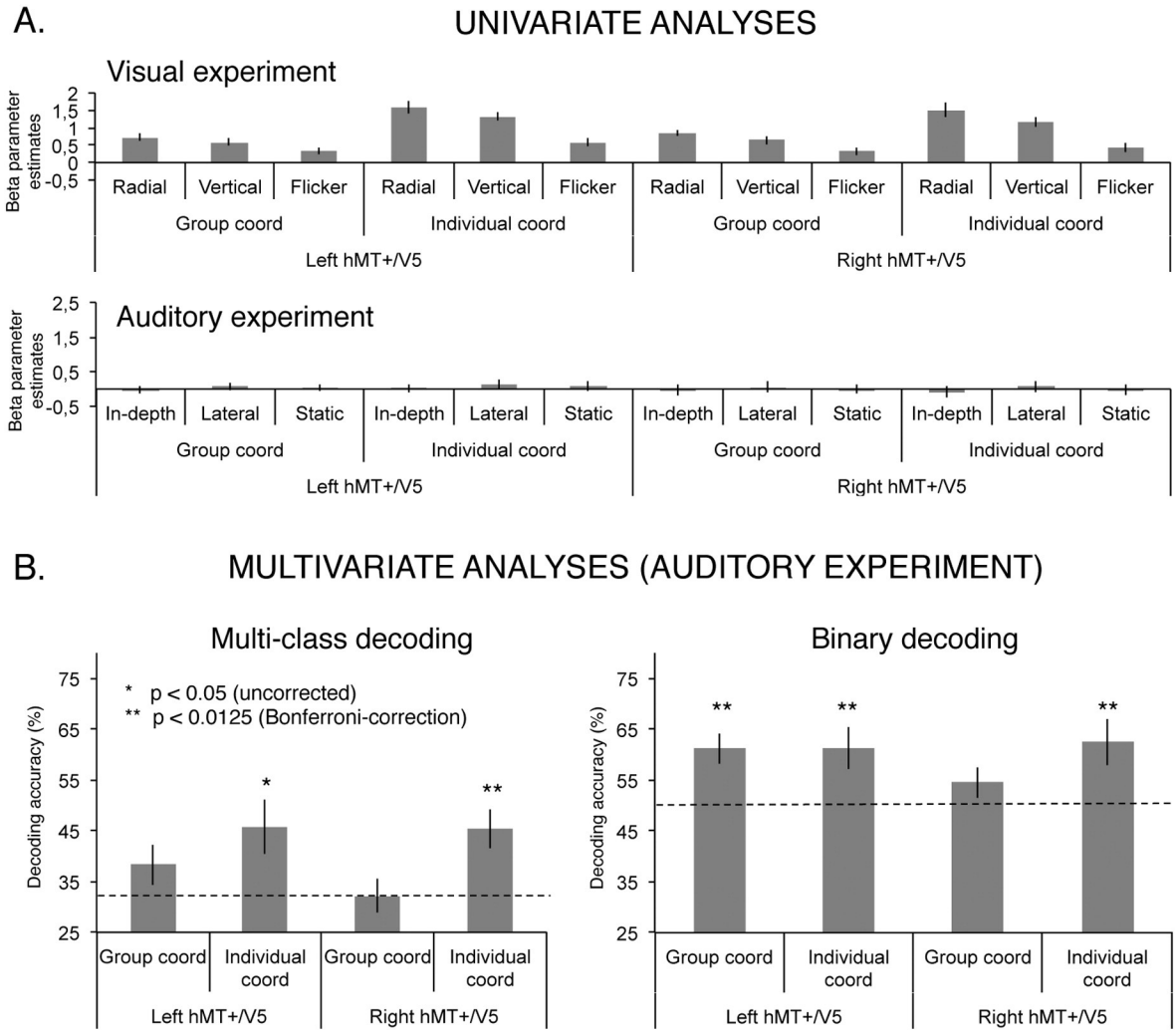

Fig. 5. Results of the regions of interest analyses (6-mm sphere) centered on group vs. individually located left and right hMT+/V5 in sighted subjects. (A) For illustration, beta parameter estimates within these regions of interest are plotted in the visual and the auditory experiments. (B) Results of the multivariate pattern analyses in the auditory experiment. Left-panel: multi-class decoding accuracy of the 3 auditory conditions (in-depth, lateral, static). Right-panel: binary decoding accuracy of the 2 auditory motion conditions (in-depth vs. lateral motion). Error bars represent standard error of the mean. Dotted line represents chance level (33.33% and 50% for multi-class and binary decoding, respectively).

assumption is supported by previous TMS studies conducted in sighted and early blind individuals. For example, TMS applied over the right intraparietal sulcus disrupted spatial localization performance only in sighted subjects (Collignon et al., 2009a). Similarly, TMS applied over the sensori-motor cortex during a tactile discrimination task strongly impaired performance in sighted subjects whereas impairment was only minor in early blind subjects (Cohen et al., 1997). Likewise, TMS applied over the prefrontal cortex during verb generation significantly increased the number of errors produced only in sighted subjects (Amedi et al., 2004). In the aforementioned studies, TMS applied over the occipital cortex systematically impaired behavioral performance in early blind subjects. Evidence from neuroimaging studies exists to demonstrate that in early blindness, such a large scale sharing of resources could be supported by strengthened cortico-cortical connections between temporal and occipital areas (Klinge et al., 2010; Collignon et al., 2013).

We conducted functional connectivity analyses targeting the right planum temporale in order to empirically test the prediction of a large-scale imbalance in the brain network supporting auditory motion processing in early blind subjects. Early blind subjects, when compared to sighted controls, showed enhanced integration between the right planum temporale and the right occipito-temporal regions and a concomitant reduced connectivity with parietal and frontal regions (Fig. 2B). These results compellingly support our suggestion that early sensory deprivation affects the balance existing between cortical areas that are part of a network that supports a given cognitive function. Early sensory deprivation appears to alter this balance by increasing the contribution of the sensory-deprived areas and decreasing the contribution of non-deprived regions that are typically involved in the same function in normally sighted subjects (Collignon et al., 2009a).

These findings raise an important question pertaining to the specific computational steps that occur in hMT+/V5 and the planum temporale during auditory motion processing in the blind. Since the duplication of computational processes between these regions would be inefficient, we speculate that these regions support distinct computational mechanisms in auditory motion processing. Understanding how developmental vision influences this reorganization is a major challenge for further research.

4.3. Decoding auditory motion content within bilateral hMT+/V5 in early blind and sighted individuals

Whole-brain searchlight MVPA analyses showed some overlap between auditory and visual decoding in occipito-temporal regions in the vicinity of hMT+/V5 even in the sighted group (Fig. 3B). Further region of interest analyses targeting visual area hMT+/V5 in the sighted revealed that this overlap of auditory and visual decoding was not simply due to group averaging (Saenz et al., 2008; Jiang et al., 2015). In fact, in individually-defined area hMT+/V5, decoding accuracy was significant

in the right hemisphere both using multi-class and binary decoding, and significant in the left hemisphere using binary decoding (Fig. 5B).

In the case of multi-class decoding, accuracy was overall higher in individually-defined coordinates than in group-defined coordinates (see Fig. 5B), suggesting that auditory motion information could be more highly decoded *within* individually defined hMT+/V5 rather than in neighboring areas (i.e. using group-level coordinate). The finding that binary classification accuracy was above chance level in individually-defined hMT+/V5 of the sighted further demonstrates that this area not only distinguishes between motion vs. static information but further contains information about different auditory motion planes.

These findings are in line with previous work suggesting that non-visual motion information is present to some extent in hMT+/V5 of subjects with typical visual experience (Hagen et al., 2002; Warren et al., 2002; Blake et al., 2004; Poirier et al., 2005; Ricciardi et al., 2007; Alink et al., 2008; Strnad et al., 2013; van Kemenade et al., 2014).

The presence of auditory motion information in areas that do not show differential activation levels in response to moving sounds reconcile previous work that used a univariate approach and failed to reveal auditory motion related responses in hMT+/V5 in sighted subjects (Lewis et al., 2000; Bremmer et al., 2001; Saenz et al., 2008; Bedny et al., 2010). This does not imply that the use of MVPA systematically provides positive findings for the presence of auditory motion information in hMT+/V5. For instance, two studies failed to reveal directional selectivity to laterally moving sounds in this area in sighted subjects (Alink et al., 2011; Jiang et al., 2014). While this might seem at odds with the present findings, it is possible that activity patterns elicited in hMT+/V5 by sounds moving laterally vs. frontally in the azimuth (present study) differ to a larger extent from activity patterns elicited by sounds moving laterally to the right vs. to the left (Alink et al., 2011; Jiang et al., 2014). In other words, different categories of sound trajectories (e.g. lateral vs. in-depth motion) might be more reliably decoded than specific sub-categorical (e.g. left vs. right) auditory motion information in hMT+/V5 of the sighted.

In line with our findings, Bedny et al. (2010) also reported no responses to auditory motion in hMT+/V5 in sighted subjects when using a univariate approach, while multivariate pattern analyses conducted on the same data set revealed that high vs. low motion content could be decoded in this area in sighted subjects (Strnad et al., 2013). Importantly, in contrast to Strnad et al. (2013) who focused their analyses on hMT+/V5, the whole brain approach adopted in the present study allows us to demonstrate that the effects observed in the sighted "visual cortex" are specific to occipito-temporal regions in the vicinity of hMT+/V5 (Fig. 3B).

Different theoretical accounts could explain the presence of non-visual motion information in a region that strongly responds to visual motion in the sighted. According to the metamodal/supramodal theory of the brain (Pascual-Leone and Hamilton, 2001; Ricciardi and Pietrini, 2011; Reich et al., 2012; Ricciardi et al., 2014), parts of hMT+/V5 may act as a supramodal processor for motion, performing motion computations independently of the modality over which it operates and developing independently of any visual experience (Ricciardi and Pietrini, 2011; Ricciardi et al., 2014). In other words, computing motion information may become abstracted from the input and from sensory experience. Our results do not fully support such a pure metamodal/supramodal assumption. First, univariate analyses showed strong visual motion selectivity in bilateral hMT+/V5 (Figs. 3A and 5A) but no response (or else a response *suppression*) to auditory motion in this area in the sighted (Figs. 2A, 3A and 5A). Second, visual experience strongly impacted on the response profile of this area, more specifically in the right hemisphere. Indeed, only the blind group showed functionally specific activity in response to auditory motion in right hMT+/V5 (Fig. 2A, Supplementary Fig. 2), and decoding accuracy for the different auditory conditions (multi-class and binary) in this region was higher in the blind than in the sighted group (Fig. 4A and B). Third, functional connectivity between hMT+/V5 and planum temporale was enhanced in early blind compared to sighted subjects (Fig. 2B), suggesting that visual experience influences this region at the network level. Altogether our findings demonstrate that hMT+/V5 responds differentially to auditory and visual motion in sighted subjects and that a lack of visual experience impacts on the response properties and on the connectivity profile of this area. Based on these observations, we suggest that, at least in the context of our experiment, hMT+/V5 does not meet all the criteria to qualify as a 'pure' supramodal region as defined above. However, our results do not reject the idea that at least some subparts of hMT+/V5 (e.g. anterior regions, see Beauchamp et al., 2007; Ricciardi et al., 2007) may present some multimodal or multisensory properties. Indeed, this region shows some overlap in decoding motion across modalities (vision and audition) and populations (sighted and blind) (Fig. 3B). This is even more apparent within individually defined hMT+/V5 in the sighted (Fig. 5B).

What might be the computational role of auditory motion information located in hMT+/V5 in the sighted? One possibility is that auditory and visual motion representations are integrated in this region. This would be consistent with the finding that area hMT+/V5 integrates dynamic information provided by different sensory modalities (Alink et al., 2008; Saldern and Noppeney, 2013) and that it responds indirectly to auditory moving sounds when congruently paired to a visual dynamic stimulus (Alink et al., 2008). It is also in accordance with psychophysiological observations that moving sounds lead to the perception of a simultaneously presented visual pattern as moving in the same direction (Jain et al., 2008; Schouten et al., 2011). The presence of auditory motion information in bilateral hMT+/V5 provides further support for the idea that crossmodal reorganization in early blind subjects may build on pre-existing intermodal connections between the auditory and the "visual" cortices in sighted subjects (Klinge et al., 2010; Collignon et al., 2013). Together with the observation that hMT+/V5 maintains its functional preference for dynamic information in case of early visual deprivation, the presence of auditory motion information in area hMT+/V5 of the sighted illustrates that crossmodal plasticity in early blindness may be constrained by innate patterns of brain architecture and connectivity (Collignon et al., 2009b; Mahon and Caramazza, 2011; Reich et al., 2012).

An alternative interpretation accounting for the presence of auditory motion information in area hMT+/V5 in sighted individuals is mental visual imagery (Goebel et al., 1998; Emmerling et al., 2015). For instance, it could be argued that hMT+/V5 supports auditory motion processing *per se* in early blind whereas it could subtend visual mental imagery in the sighted. While no study to date can conclusively rule it out, the reliance on visual imagery is unlikely to account for the pattern of results observed in the sighted in the present study. First, we specifically selected auditory stimuli that elicit low imagery content (noise). Second, mental visual imagery of motion was previously shown to increase overall response in hMT+/V5 (Goebel et al., 1998; Emmerling et al., 2015), while no such difference in activation levels was found in the sighted group in the univariate analyses.

4.4. Limitations and perspectives

Inconsistencies between studies regarding non-visual motion responses in hMT+/V5 in the sighted (see Section 1) may stem from a variety of parameters. In addition to the choice of analytical steps (univariate, multivariate, whole brain or regions of interest) that we have addressed in the present study, other important parameters concern the sensory modality investigated (audition vs. touch), the specific features of the stimuli (e.g. interaural level or time differences for moving sounds) and the implemented experimental paradigm (e.g. block vs. event-related design).

A major difference between the present study and previous investigations is the use of auditory stimuli instead of tactile ones (eg. Ricciardi et al., 2007; Beauchamp et al., 2007; Jiang et al., 2015). As stimuli conveyed by different sensory organs also possess specific psychophysical

characteristics, it is likely that the involvement of hMT+/V5 for non-visual motion processing depends on the input modality (auditory vs. tactile). Although some work has been carried out on the topic (e.g. Bremmer et al., 2001), a direct comparison of auditory and tactile motion processing using carefully controlled stimuli represents an interesting avenue for future studies.

To characterize the nature of hMT+/V5 involvement in non-visual motion processing, one should go beyond reporting overlapping activations or decoding accuracy between modalities or populations. Given the resolution of fMRI, overlapping functional activations elicited by distinct sensory modalities may reflect the recruitment of supramodal neurons, or the recruitment of different unimodal neuronal populations (Ricciardi and Pietrini, 2011). In order to potentially localize those cortical regions that functionally contribute to a supramodal representation, multivariate analysis can be used to classify neural responses across sensory modalities and experimental samples (e.g., blind and sighted). Our design does not allow such investigation due to the lack of pure correspondence between the stimuli used in the auditory and visual modalities (i.e. vertically moving patterns versus laterally moving sounds; see Section 2.2.2 for arguments supporting the use of different motion planes across modalities). Aside from cross-modal (auditory–visual) decoding in the sighted, cross-group decoding represents an additional challenge since the multivariate representational space of a specific stimulus varies dramatically across participants. Therefore, to achieve reliable cross-subject (and therefore cross-groups) decoding, it is important to rely on specific methods to align participants in a similar functional space (Haxby et al., 2011).

Our paradigm prevents the decoding of different motion trajectories within the same plane (i.e. left vs. right, looming vs. receding moving sounds). The latter would have necessitated the use of an event-related design or a block design presenting different motion trajectories in separate blocks (eg. Alink et al., 2011). The block design used in the present study aimed at minimizing adaptation effects related to the presentation of a stimulus in the same direction, thus increasing statistical power and maximizing the possibility to detect auditory motion information even in the visual cortex of sighted subjects. Moreover, this paradigm allowed us to investigate preferential tuning for separate motion planes as previously reported in vision (e.g. Morrone et al., 2000). Some studies have attempted to characterize the functional properties of hMT+/V5 in the early blind by decoding different motion trajectories in this area and have provided interesting positive findings (Wolbers et al., 2011, Jiang et al., 2014). These types of studies combined with a cross-modal and cross-subject decoding approach have the promise to reveal important insights about the nature of the auditory motion information content rooted in classically considered 'visual' regions in both sighted and early blind individuals.

4.5. Conclusions

Using a combination of univariate and multivariate pattern analyses at the whole brain level, the present study demonstrates that developmental vision shapes brain areas supporting the computation of auditory and visual motion. We show that auditory motion selectivity in the reorganized occipital cortex of the blind is confined to right occipito-temporal regions, overlapping with regions that are selective to visual motion in the sighted. These results support and extend the view that in the absence of vision since birth, hMT+/V5 maintains its functional preference for computing motion information while reorienting its modality tuning toward the preserved non-visual modalities (see Bedny et al., 2010; Collignon et al., 2011; Reich et al., 2011 for similar findings of a maintenance of functional selectivity in the blind). The more subtle presence of auditory-motion related information found in area hMT+/V5 of the sighted supports the idea that crossmodal reorganization in case of early visual deprivation may build on pre-existing connections between the auditory and the visual cortex in sighted individuals. Crucially, using multivariate decoding of different sound motion conditions we demonstrate that this crossmodal reorganization triggers a large-scale imbalance between auditory and "visual" brain regions typically supporting the processing of motion information, by increasing the reliance on "visual" areas and decreasing the reliance on auditory areas.

Conflict of interest

The authors declare no conflict of interest.

Acknowledgments

This work was supported by the Canada Research Chair Program (FL), the Canadian Institutes of Health Research (FL), the Belgian National Fund for Scientific Research (GD) and a European Research Council starting grant (MADVIS grant #337573) attributed to OC.

Appendix A. Supplementary material

Supplementary data to this article can be found online at http://dx.doi.org/10.1016/j.neuroimage.2016.04.027.

References

Alink, A., Singer, W., Muckli, L., 2008. Capture of auditory motion by vision is represented by an activation shift from auditory to visual motion cortex. J. Neurosci. 28, 2690–2697.
Alink, A., Euler, F., Kriegeskorte, N., Singer, W., Kohler, A., 2011. Auditory motion direction encoding in auditory cortex and high-level visual cortex. Hum. Brain Mapp. 33, 969–978.
Amedi, A., Floel, A., Knecht, S., Zohary, E., Cohen, L.G., 2004. Transcranial magnetic stimulation of the occipital pole interferes with verbal processing in blind subjects. Nat. Neurosci. 7, 1266–1270.
Ashburner, J., 2007. A fast diffeomorphic image registration algorithm. NeuroImage 38, 95–113.
Beauchamp, M.S., Yasar, N.E., Kishan, N., Ro, T., 2007. Human MST but not MT responds to tactile stimulation. J. Neurosci. 27, 8261–8267.
Bedny, M., Konkle, T., Pelphrey, K., Saxe, R., Pascual-Leone, A., 2010. Sensitive period for a multimodal response in human visual motion area MT/MST. Curr. Biol. 20, 1900–1906.
Bedny, M., Richardson, H., Saxe, R., 2015. "Visual" cortex responds to spoken language in blind children. J. Neurosci. 35, 11674–11681.
Blake, R., Sobel, K.V., James, T.W., 2004. Neural synergy between kinetic vision and touch. Psychol. Sci. 15, 397–402.
Bremmer, F., Schlack, A., Shah, N.J., Zafiris, O., Kubischik, M., Hoffmann, K., Zilles, K., Fink, G.R., 2001. Polymodal motion processing in posterior parietal and premotor cortex: a human fMRI study strongly implies equivalencies between humans and monkeys. Neuron 29, 287–296.
Cohen, L.G., Celnik, P., Pascual-Leone, A., Corwell, B., Falz, L., Dambrosia, J., Honda, M., Sadato, N., Gerloff, C., Catalá, M.D., Hallett, M., 1997. Functional relevance of cross-modal plasticity in blind humans. Nature 389, 180–183.
Collignon, O., Lassonde, M., Lepore, F., Bastien, D., Veraart, C., 2007. Functional cerebral reorganization for auditory spatial processing and auditory substitution of vision in early blind subjects. Cereb. Cortex 17, 457–465.
Collignon, O., Davare, M., Olivier, E., De Volder, A.G., 2009a. Reorganisation of the right occipito-parietal stream for auditory spatial processing in early blind humans. A transcranial magnetic stimulation study. Brain Topogr. 21, 232–240.
Collignon, O., Voss, P., Lassonde, M., Lepore, F., 2009b. Cross-modal plasticity for the spatial processing of sounds in visually deprived subjects. Exp. Brain Res. 192, 343–358.
Collignon, O., Vandewalle, G., Voss, P., Albouy, G., Charbonneau, G., Lassonde, M., Lepore, F., 2011. Functional specialization for auditory–spatial processing in the occipital cortex of congenitally blind humans. Proc. Natl. Acad. Sci. U. S. A. 108, 4435–4440.
Collignon, O., Dormal, G., Albouy, G., Vandewalle, G., Voss, P., Phillips, C., Lepore, F., 2013. Impact of blindness onset on the functional organization and the connectivity of the occipital cortex. Brain 136, 2769–2783.
Corbetta, M., Shulman, G.L., 2002. Control of goal-directed and stimulus-driven attention in the brain. Nat. Rev. Neurosci. 3, 201–215.
Dumoulin, S.O., Bittar, R.G., Kabani, N.J., Baker, C.L., Le Goualher, G., Bruce Pike, G., Evans, A.C., 2000. A new anatomical landmark for reliable identification of human area V5/MT: a quantitative analysis of sulcal patterning. Cereb. Cortex 10, 454–463.
Elbert, T., Sterr, A., Rockstroh, B., Pantev, C., Müller, M.M., Taub, E., 2002. Expansion of the tonotopic area in the auditory cortex of the blind. J. Neurosci. 22, 9941–9944.
Emmerling, T.C., Zimmermann, J., Sorger, B., Frost, M.A., Goebel, R., 2015. Decoding the direction of imagined visual motion using 7T ultra-high field fMRI. NeuroImage 125, 61–73.
Gitelman, D.R., Penny, W.D., Ashburner, J., Friston, K.J., 2003. Modeling regional and psychophysiologic interactions in fMRI: the importance of hemodynamic deconvolution. NeuroImage.
Goebel, R., Khorram-Sefat, D., Muckli, L., Hacker, H., Singer, W., 1998. The constructive nature of vision: direct evidence from functional magnetic resonance imaging studies of apparent motion and motion imagery. Eur. J. Neurosci. 10, 1563–1573.

Gougoux, F., Belin, P., Voss, P., Lepore, F., Lassonde, M., Zatorre, R.J., 2009. Voice perception in blind persons: a functional magnetic resonance imaging study. Neuropsychologia 47, 2967–2974.
Griffiths, T.D., Green, G.G., 1999. Cortical activation during perception of a rotating wide-field acoustic stimulus. NeuroImage 10, 84–90.
Griffiths, T.D., Green, G.G., Rees, A., Rees, G., 2000. Human brain areas involved in the analysis of auditory movement. Hum. Brain Mapp. 9 (2), 72–80.
Hagen, M.C., Franzen, O., McGlone, F., Essick, G., Dancer, C., Pardo, J.V., 2002. Tactile motion activates the human middle temporal/V5 (MT/V5) complex. Eur. J. Neurosci. 16, 957–964.
Hart, H.C., Palmer, A.R., Hall, D.A., 2004. Different areas of human non-primary auditory cortex are activated by sounds with spatial and nonspatial properties. Hum. Brain Mapp. 21, 178–190.
Haxby, J.V., Guntupalli, J.S., Connolly, A.C., Halchenko, Y.O., Conroy, B.R., Gobbini, M.I., Hanke, M., Ramadge, P.J., 2011. A common, high-dimensional model of the representational space in human ventral temporal cortex. Neuron 72, 404–416.
Hölig, C., Föcker, J., Best, A., Röder, B., Büchel, C., 2014. Brain systems mediating voice identity processing in blind humans. Hum. Brain Mapp. 35, 4607–4619.
Huk, A.C., Dougherty, R.F., Heeger, D.J., 2002. Retinotopy and functional subdivision of human areas MT and MST. J. Neurosci. 22, 7195–7205.
Jain, A., Sally, S.L., Papathomas, T.V., 2008. Audiovisual short-term influences and aftereffects in motion: examination across three sets of directional pairings. J. Vis. 8, 7.1–7.13.
Jiang, J., Zhu, W., Shi, F., Liu, Y., Li, J., Qin, W., 2009. Thick visual cortex in the early blind. J. Neurosci. 29 (7), 2205–2211.
Jiang, F., Stecker, G.C., Fine, I., 2014. Auditory motion processing after early blindness. J. Vis. 14 (13), 4.
Jiang, F., Beauchamp, M.S., Fine, I., 2015. Re-examining overlap between tactile and visual motion responses within hMT+ and STS. NeuroImage 119, 187–196.
Klein, M.E., Zatorre, R.J., 2014. Representations of invariant musical categories are decodable by pattern analysis of locally distributed BOLD responses in superior temporal and intraparietal sulci. Cereb. Cortex 25 (7), 1947–1957.
Klinge, C., Eippert, F., Röder, B., Büchel, C., 2010. Corticocortical connections mediate primary visual cortex responses to auditory stimulation in the blind. J. Neurosci. 30, 12798–12805.
Kriegeskorte, N., Goebel, R., Bandettini, P., 2006. Information-based functional brain mapping. Proc. Natl. Acad. Sci. U. S. A. 103, 3863–3868.
Lewald, J., Getzmann, S., 2013. Ventral and dorsal visual pathways support auditory motion processing in the blind: evidence from electrical neuroimaging. Eur. J. Neurosci. 38, 3201–3209.
Lewis, J.W., Beauchamp, M.S., DeYoe, E.A., 2000. A comparison of visual and auditory motion processing in human cerebral cortex. Cereb. Cortex 10, 873–888.
Mahon, B.Z., Caramazza, A., 2011. What drives the organization of object knowledge in the brain? Trends Cogn. Sci. (Regul. Ed.) 15, 97–103.
Morrone, M.C., Tosetti, M., Montanaro, D., Fiorentini, A., Cioni, G., Burr, D.C., 2000. A cortical area that responds specifically to optic flow, revealed by fMRI. Nat. Neurosci. 3, 1322–1328.
Noppeney, U., Friston, K.J., Ashburner, J., Frackowiak, R., Price, C.J., 2005. Early visual deprivation induces structural plasticity in gray and white matter. Curr. Biol. 15, R488–R490.
Oosterhof, N.N., Connolly, A.C., Haxby, J.V., 2016. CoSMoMVPA: Multi-modal Multivariate Pattern Analysis of Neuroimaging Data in Matlab/GNU Octave, http://biorxiv.org. http://dx.doi.org/10.1101/047118.
Pan, W.-J., Wu, G., Li, C.-X., Lin, F., Sun, J., Lei, H., 2007. Progressive atrophy in the optic pathway and visual cortex of early blind Chinese adults: a voxel-based morphometry magnetic resonance imaging study. NeuroImage 37, 212–220.
Park, H.-J., Lee, J.D., Kim, E.Y., Park, B., Oh, M.-K., Lee, S., Kim, J.-J., 2009. Morphological alterations in the congenital blind based on the analysis of cortical thickness and surface area. NeuroImage 47, 98–106.
Pascual-Leone, A., Hamilton, R., 2001. The metamodal organization of the brain. Prog. Brain Res. 134, 427–445.
Pavani, F., Macaluso, E., Warren, J.D., Driver, J., Griffiths, T.D., 2002. A common cortical substrate activated by horizontal and vertical sound movement in the human brain. Curr. Biol. 12, 1584–1590.
Petrides, M., 2012. The Human Cerebral Cortex: An MRI Atlas of the Sulci and Gyri in MNI Stereotaxic Space.
Poirier, C., Collignon, O., Devolder, A.G., Renier, L., Vanlierde, A., Tranduy, D., Scheiber, C., 2005. Specific activation of the V5 brain area by auditory motion processing: an fMRI study. Brain Res. Cogn. Brain Res. 25, 650–658.
Poirier, C., Collignon, O., Scheiber, C., Renier, L., Vanlierde, A., Tranduy, D., Veraart, C., De Volder, A.G., 2006. Auditory motion perception activates visual motion areas in early blind subjects. NeuroImage 31, 279–285.
Reich, L., Szwed, M., Cohen, L., Amedi, A., 2011. A ventral visual stream reading center independent of visual experience. Curr. Biol. 21, 363–368.
Reich, L., Maidenbaum, S., Amedi, A., 2012. The brain as a flexible task machine: implications for visual rehabilitation using noninvasive vs. invasive approaches. Curr. Opin. Neurol. 25 (1), 86–95.
Ricciardi, E., Pietrini, P., 2011. New light from the dark: what blindness can teach us about brain function. Curr. Opin. Neurol. 24, 357–363.
Ricciardi, E., Vanello, N., Sani, L., Gentili, C., Scilingo, E.P., Landini, L., Guazzelli, M., Bicchi, A., Haxby, J.V., Pietrini, P., 2007. The effect of visual experience on the development of functional architecture in hMT+. Cereb. Cortex 17, 2933–2939.
Ricciardi, E., Bonino, D., Pellegrini, S., Pietrini, P., 2014. Mind the blind brain to understand the sighted one! Is there a supramodal cortical functional architecture? Neurosci. Biobehav. Rev. 41, 64–77.
Saenz, M., Lewis, L.B., Huth, A.G., Fine, I., Koch, C., 2008. Visual motion area MT+/V5 responds to auditory motion in human sight-recovery subjects. J. Neurosci. 28, 5141–5148.
Saito, H., Yukie, M., Tanaka, K., Hikosaka, K., Fukada, Y., Iwai, E., 1986. Integration of direction signals of image motion in the superior temporal sulcus of the macaque monkey. J. Neurosci. 6, 145–157.
Saldern, v.S., Noppeney, U., 2013. Sensory and striatal areas integrate auditory and visual signals into behavioral benefits during motion discrimination. J. Neurosci. 33, 8841–8849.
Schouten, B., Troje, N.F., Vroomen, J., Verfaillie, K., 2011. The effect of looming and receding sounds on the perceived in-depth orientation of depth-ambiguous biological motion figures. PLoS One 6, e14725.
Seifritz, E., Neuhoff, J.G., Bilecen, D., Scheffler, K., Mustovic, H., Schächinger, H., Elefante, R., Di Salle, F., 2002. Neural processing of auditory looming in the human brain. Curr. Biol. 12, 2147–2151.
Sterr, A., Müller, M.M., Elbert, T., Rockstroh, B., Pantev, C., Taub, E., 1998a. Changed perceptions in Braille readers. Nature 391, 134–135.
Sterr, A., Müller, M.M., Elbert, T., Rockstroh, B., Pantev, C., Taub, E., 1998b. Perceptual correlates of changes in cortical representation of fingers in blind multifinger Braille readers. J. Neurosci. 18, 4417–4423.
Stevens, A.A., Weaver, K.E., 2009. Functional characteristics of auditory cortex in the blind. Behav. Brain Res. 196, 134–138.
Strnad, L., Peelen, M.V., Bedny, M., Caramazza, A., 2013. Multivoxel pattern analysis reveals auditory motion information in MT+ of both congenitally blind and sighted individuals. PLoS One 8, e63198.
Stumpf, E., Toronchuk, J.M., Cynader, M.S., 1992. Neurons in cat primary auditory cortex sensitive to correlates of auditory motion in three-dimensional space. Exp. Brain Res. 88, 158–168.
Summers, I.R., Francis, S.T., Bowtell, R.W., McGlone, F.P., Clemence, M., 2009. A functional-magnetic-resonance-imaging investigation of cortical activation from moving vibrotactile stimuli on the fingertip. J. Acoust. Soc. Am. 125, 1033–1039.
Sunaert, S., Van Hecke, P., Marchal, G., Orban, G.A., 1999. Motion-responsive regions of the human brain. Exp. Brain Res. 127, 355–370.
Tanaka, K., Saito, H., 1989. Analysis of motion of the visual field by direction, expansion/contraction, and rotation cells clustered in the dorsal part of the medial superior temporal area of the macaque monkey. J. Neurophysiol. 62, 626–641.
Tootell, R.B., Reppas, J.B., Kwong, K.K., Malach, R., Born, R.T., Brady, T.J., Rosen, B.R., Belliveau, J.W., 1995. Functional analysis of human MT and related visual cortical areas using magnetic resonance imaging. J. Neurosci. 15, 3215–3230.
Toronchuk, J.M., Stumpf, E., Cynader, M.S., 1992. Auditory cortex neurons sensitive to correlates of auditory motion: underlying mechanisms. Exp. Brain Res. 88, 169–180.
van Kemenade, B.M., Seymour, K., Wacker, E., Spitzer, B., Blankenburg, F., Sterzer, P., 2014. Tactile and visual motion direction processing in hMT+/V5. NeuroImage 84, 420–427.
Warren, J.D., Zielinski, B.A., Green, G.G.R., Rauschecker, J.P., Griffiths, T.D., 2002. Perception of sound-source motion by the human brain. Neuron 34, 139–148.
Watkins, K.E., Shakespeare, T.J., O'Donoghue, M.C., Alexander, I., Ragge, N., Cowey, A., Bridge, H., 2013. Early auditory processing in area V5/MT+ of the congenitally blind brain. J. Neurosci. 33, 18242–18246.
Watson, J.D., Myers, R., Frackowiak, R.S., Hajnal, J.V., Woods, R.P., Mazziotta, J.C., Shipp, S., Zeki, S., 1993. Area V5 of the human brain: evidence from a combined study using positron emission tomography and magnetic resonance imaging. Cereb. Cortex 3, 79–94.
Weeks, R., Horwitz, B., Aziz-Sultan, A., Tian, B., Wessinger, C.M., Cohen, L.G., Hallett, M., Rauschecker, J.P., 2000. A positron emission tomographic study of auditory localization in the congenitally blind. J. Neurosci. 20, 2664–2672.
Wolbers, T., Zahorik, P., Giudice, N.A., 2011. Decoding the direction of auditory motion in blind humans. NeuroImage 56, 681–687.